

Response to reviewers

Reviewers comments are in black, our responses are in red

Reviewer 1

First, the largest issue I see is still minor. The new LiDAR data in the Guatemalan Biosphere Reserve is given a lot of credit (page 8 lines 114-117). However, that project has yet to produce a peer reviewed article on their dataset. While Inomata works in Guatemala (and is a good reference) he was not part of that LiDAR consortium. The Guatemalan data has made some drastic statements, but until they manage to pass peer review, I might not give them so much credit ... yet. While the data will certainly impact interpretations, it does a disservice to other scholars in the region who have already used LiDAR data to advance our understanding of the Maya (such as Prufer and Thompson already cited later in the paper). I could recommend other citations here as well, but they aren't absolutely necessary to the paper. Instead, on page 8 lines 114-117. Would you consider separating the list of LiDAR study areas? Most of those papers do not cover Guatemalan LiDAR data, so instead I would recommend something along the lines of this in place of "see also", "... as has the past decade of LiDAR use worldwide" followed by the non-Guatemalan LiDAR citations. This will at least highlight the impact of previous research along with the new research out of Guatemala, even if Inomata's article is from a separate LiDAR project.

The project from Guatemala was finally published in October (Canuto et al, 2018) which we have now cited in conjunction with the other references. With the addition of this reference, we have also modified the citations on page 8 with accordance to the suggestions of the reviewer. After citing the Guatemala case study, we include "This is accompanied by a decade of LiDAR studies worldwide" followed by the string of related citations.

As an addition to Evans on page 4 line 62, I would also recommend citing the following reference, which describes LiDAR use in archaeology in a historical context.

We have added the reference to Chase et al. (2017) as suggested by the reviewer.

On page 8 line 118. There are algorithms used for LiDAR analysis that create alternative visualizations. As such, could you change the line to "Two general classes of automated detection algorithms exist ..."

We have rephrased the sentence as suggested by the reviewer.

On page 15, line 255. Could you please provide the specific inputs used for the Focal Statistics tool (shape and size used probably) and include the version of ArcGIS used for this analysis?

The inputs and the version of ArcGIS have been added to the sentence.

On page 26-27, lines 393-403. What is the minimum feature size that you would expect to be able to identify through the four methods provided? How does the quality of the

input dataset/DEM affect the size of detectable objects? If this comment is too difficult to answer in text, then absolutely feel free to ignore it.

Our methods and datasets allow us to detect “features as small as a few meters across and about half-a-meter tall” (lines 403-404). The second question regarding quality and its effect on the detection of different sized objects is addressed in the following paragraph on lines 409-410 “Increasing the ability to detect smaller features requires higher resolution dataset: greater the spatial resolution, the smaller the objects that can be detected.”

#### Reviewer 2

- LINE 26: The Howe,2014 reference may not be the most authoritative source to estimate the number of mounds in the eastern US. Just saying "thousands" get the point across. If you would like to suggest a higher number perhaps some additional citations might bolster this claim.

We have changed the sentence to say “thousands” as suggested by the reviewer and we have added several other sources in addition to Howe (2014).

LINE 61,62: "Active sensors, such as light detecting and ranging (LiDAR), offer maps of topography (Evans et al., 2013)" It's not just the ability to map the terrain, but a non-bias topographic mapping technique, which is substantially different (and much quicker) than traditional total station mapping.

We have rephrased the sentence to include this information. It now reads: “Active sensors, such as light detecting and ranging (LiDAR), provide a mapping technique that permits direct measurements of surface topography that is faster, more systematic, and more accurate than other forms of manual mapping.”

LINE 214: In the section on Template Matching it appears that the target objects are switched to only pre-contact mounds? Are the shell rings and other archaeological features eschewed for this methodology?

We have rephrased the statement to include the fact that rings are included in this template dataset. Both shell rings and earthen/shell mound features in the study areas are included in these templates. The statement now reads as “We created templates using a selection of 29 mound and ring features using characteristics of elevation, slope, focal statistics, and openness.” (lines 218-220).

GENERAL: Standardize formatting in all figures. Legends, scales and text font are not consistent.

The formatting of all legends and fonts has been standardized for all figures. In instances of different scaling for different panels of a figure, multiple scale-bars are used to indicate the difference.

GENERAL: Would be interesting to provide a comparison between the computer algorithmic detection and manual detection for at least one of the areas. Does a human operator provide fewer false positives or would they miss a number of features the algorithms detect?

We added a paragraph to our discussion/conclusion section which briefly goes over some comparisons between manual evaluation and automatic evaluation in this area (lines 419-429). Most of the features used for our template process were identified via manual evaluation in the LiDAR datasets. But within these same areas in Beaufort County the automated algorithms identified many other confirmed sites that were not picked out via manual means.

Highlights

- 4 different automatic detection methods are examined
- Segmentation, inverse depression analysis, template matching, combined method
- Most effective method of mound detection combines segmentation and template matching
- Inverse Depression Analysis is highly effective with several hundred iterations
- Template matching can reduce false positives resulting from natural features
- A previously unknown shell ring is identified using the proposed OBIA approach

A comparison of automated object extraction methods for mound and shell-ring identification in coastal South Carolina

October 24, 2018

Dylan S. Davis,<sup>1\*</sup> Carl P. Lipo,<sup>2</sup> and Matthew C. Sanger<sup>2</sup>

<sup>1</sup> Department of Anthropology, The Pennsylvania State University, 403 Carpenter Building, University Park, PA 16802

<sup>2</sup> Department of Anthropology, Binghamton University, 4400 Vestal Parkway, Binghamton, NY 13902

\*Corresponding Author details: [dsd40@psu.edu](mailto:dsd40@psu.edu)

1 **Abstract**

2 One persistent archaeological challenge is the generation of systematic documentation for the  
3 extant archaeological record at the scale of landscapes. Often our information for landscapes is  
4 the result of haphazard and patchy surveys that stem from opportunistic and historic efforts.  
5 Consequently, overall knowledge of some regions is the product of *ad hoc* survey area  
6 delineation, degree of accessibility, effective ground visibility, and the fraction of areas that have  
7 survived destruction from development. These factors subsequently contribute unknown biases  
8 to our understanding of chronology, settlements patterns, interaction, and exchange. Aerial  
9 remote sensing offers one potential solution for improving our knowledge of landscapes. With  
10 sensors that include LiDAR, remote sensing can identify archaeological features that are  
11 otherwise obscured by vegetation. Object-based image analyses (OBIA) of remote sensing data  
12 hold particular promise to facilitate regional analyses thorough the automation of archaeological  
13 feature recognition. Here, we explore four OBIA algorithms for artificial mound feature  
14 detection using LiDAR from Beaufort County, South Carolina: multiresolution segmentation,  
15 inverse depression analysis, template matching, and a newly designed algorithm that combines  
16 elements of segmentation and template matching. While no single algorithm proved to be  
17 consistently superior to the others, a combination of methods is shown to be the most effective  
18 for detecting archaeological features.

19

20 Keywords: Object based image analysis, template matching, automatic feature identification,  
21 remote sensing, shell rings, LiDAR, American Southeast

22

23

## 24 1.1 INTRODUCTION

25           At the time of European arrival into Eastern North America, the archaeological record  
26 included thousands of intact earth and shell mound structures (Anderson, 2012; Howe, 2014;  
27 Thomas, 1894). Beginning in the 19<sup>th</sup> century, these deposits became the focus of archaeological  
28 research due to their ability to produce artifacts that shed light on cultural affinity and  
29 chronology (Lyman et al. 1997; e.g., Claflin, 1931; Fairbanks, 1942; Ford and Willey, 1941;  
30 Jones et al., 1933; Moore, 1894a, 1894b, 1899; Moorehead, 1891; Putnam, 1875; Squier and  
31 Davis, 1848; Swallow, 1858; Wauchope, 1948; Willey, 1939). Over time, archaeological interest  
32 in mounds has grown to include studies of pre-contact technology, diet, social behavior, trade,  
33 exchange, interaction, and settlement (e.g., Anderson, 2004; Caldwell, 1952; Calmes, 1967;  
34 Claassen, 1986, 1991, 2010; Crusoe and DePratter, 1976; Marquardt, 2010; Matteson, 1960;  
35 Russo, 2004, 2006; Thompson et al., 2011; Trinkley, 1985).

36           Our knowledge of the distribution of mound features, however, tends to be biased  
37 towards some areas more than others. These areas may come from regions that have seen a  
38 greater number of field studies (e.g., Michie's (1980) survey of the coastal plains of the Port  
39 Royal Sound) but also include those that are easier to survey due to a lack of substantial ground  
40 cover such as in areas of beaches and shallow intertidal zones (South, 1960) as well as piedmonts  
41 and coastal plains (House and Ballinger, 1976). Specifically, environments that are dominated by  
42 heavy vegetation (e.g., woodlands, bayous, and coastal marshes) are often missing from our  
43 knowledge of the record as they are difficult to evaluate using systematic pedestrian tactics. The  
44 most recent example of this lapse in knowledge is the discovery of thousands of monumental  
45 complexes in the dense forests of Guatemala (Canuto et al., 2018). Prior to the use of LiDAR

46 survey, these archaeological features were unknown, and their discovery may rewrite the history  
47 of this area.

48         This aspect of past archaeological surveys raises the possibility that our knowledge of the  
49 record is biased towards features that appear in the best cleared and most visible landscapes  
50 (Banning et al., 2017; Bintliff, 2000; Bintliff et al., 1999; Hirth, 1978; Nance 1979; Stark and  
51 Garraty, 2008). The potential for increasing our understanding of the archaeological record is  
52 likely greatest in the exploration of areas that have seen little systematic observation. Given that  
53 unknown deposits are often least visited and impacted, those that remain hidden in vegetation  
54 potentially hold some of the most promising opportunities for new archaeological discovery. To  
55 address the challenges of large-scale documentation presented by heavily-vegetated landscapes,  
56 and to aid in the study of these poorly studied regions, new kinds of techniques are required.

57         Remote sensing using computational algorithms for automatic feature detection offers  
58 one promising solution. High-resolution aerial imagery provides detailed information about the  
59 structure of landscapes. Multispectral imagery expands the wavelengths that can be used for  
60 sensing to include bands that are sensitive to vegetation and sediment composition (Jensen,  
61 2007). Active sensors, such as light detecting and ranging (LiDAR), provide a mapping  
62 technique that permits direct measurements of surface topography that is faster, more systematic,  
63 and more accurate than other forms of manual mapping (Chase et al., 2017; Evans et al., 2013).  
64 New computational methods greatly facilitate the use of these many classes of data as they can  
65 be configured to automatically identify features of interest (Freeland et al., 2016; Magnini et al.,  
66 2016; Sevara et al., 2016; Trier et al., 2015). Object-based image analysis (OBIA) covers a broad  
67 array of promising algorithms for archaeological prospection (Sevara et al., 2016). These

68 compositional techniques include shape templates (Kvamme, 2013; Trier et al., 2008), machine  
69 learning algorithms (Wu et al., 2015, 2016), and image segmentation (Witharana et al., 2018).

70 Here, we evaluate an application of four OBIA methods – multiresolution segmentation,  
71 inverse depression analysis, template matching, and a method combining segmentation and  
72 template matching – as tools for identifying artificial mounds and rings. In our example  
73 applications, we make use of LiDAR data from coastal South Carolina. Our goal is to compare  
74 the results obtained by implementing these methods on a single shared set of data. In this way,  
75 the results can provide suggestions for the best practices in the use of these remote sensing tools  
76 for documenting the archaeological record.

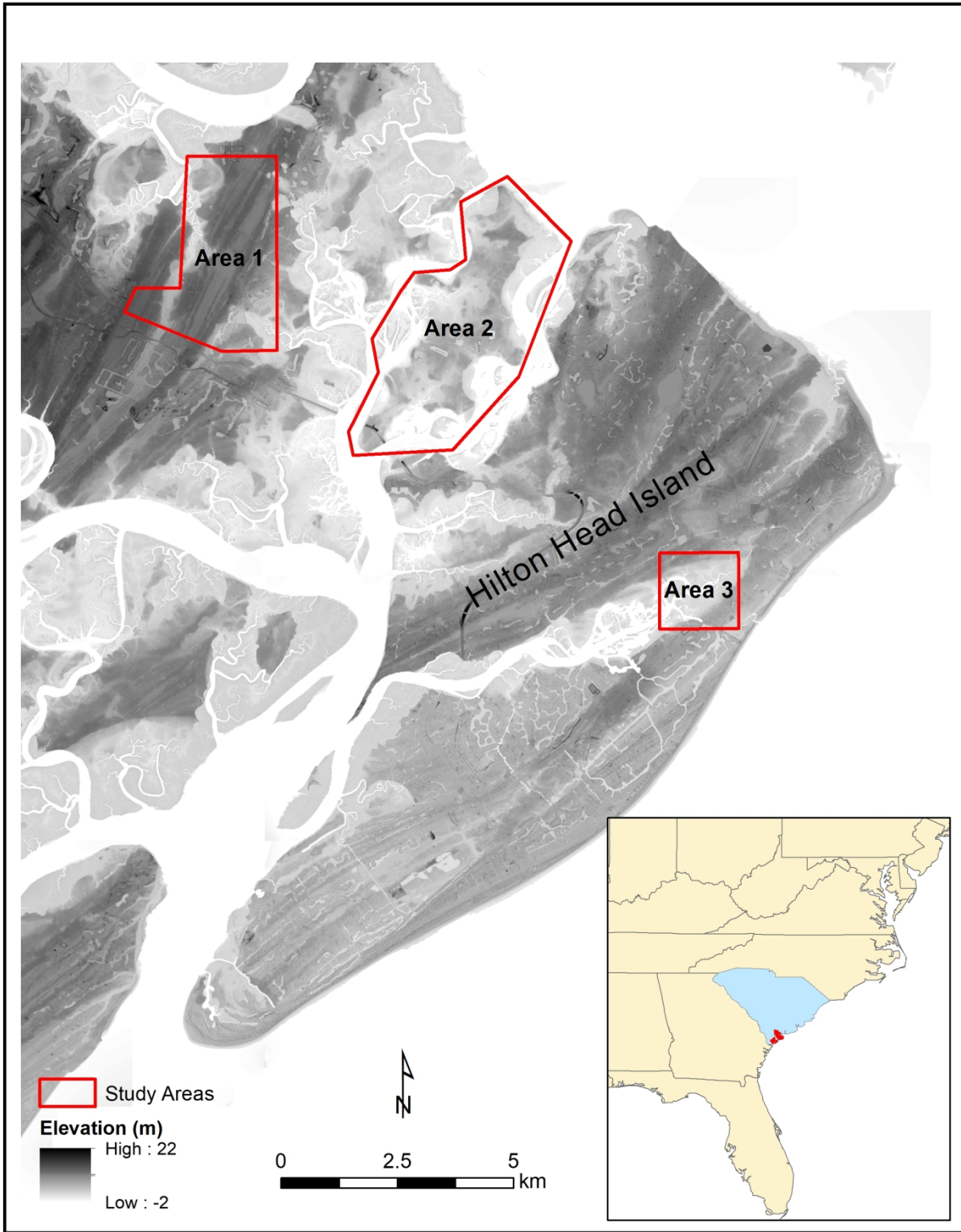
## 77 *1.2 Study Area*

78 The coastal plains of South Carolina contain a rich archaeological record but have been  
79 subjected to only limited ground surveys due to the prominence of forests and bayous (Anderson  
80 et al., 2017). Beaufort County, South Carolina, in particular, contains one of the largest number  
81 of recognized archaeological deposits in the state, a significant number of which are mound  
82 features (Frierson, 2000; Stephenson, 1971). A majority of the area, however, is densely  
83 vegetated and only limited systematic surface surveys having been conducted (e.g., Michie,  
84 1980; South, 1960, 1976).

85 The lack of systematic surveys in the region is more than an academic issue. By 2040,  
86 warming due to climate change will result in the submergence of 30,000 acres of presently dry  
87 land in this area (NOAA, 2015; see also Anderson et al., 2017). The effects of sea-level change,  
88 combined with recent urban development and population increases will potentially result in the  
89 loss of many archaeological deposits before they can be recognized. In this way, the application

90 of new approaches for rapid assessment of the otherwise hidden landscape of Beaufort County is  
91 particularly urgent.

92 To evaluate the potential of new remote sensing approaches, we chose three study areas  
93 in Beaufort County (Figure 1). Areas 1 (Victoria Bluff Heritage Preserve) and 2 (Pinckney Island  
94 Wildlife Refuge) consist of a total of 25 km<sup>2</sup> of forested land. Area 3 is composed of 3 km<sup>2</sup> of  
95 land on Hilton Head Island. These areas were chosen for evaluation based on the presence of  
96 known features, public access, and the availability of high resolution remote sensing data.



97

98 Figure 1: Study Area in Beaufort County, SC (Color online).

## 99 2.1 OBJECT-BASED IMAGE ANALYSIS (OBIA)

100 Aerial imagery has long provided archaeologists a source of information for studying  
101 archaeological features across landscapes in an efficient and cost-effective fashion (e.g., Agache,  
102 1968; Bradford, 1956; Buettner-Januch, 1954; Campbell, 1981; Capper, 1907; Drager, 1983;  
103 Engelbach, 1929; Harp, 1966; Lindbergh, 1929a, 1929b; Madry and Crumley, 1990; McKinley,  
104 1921; Parrington, 1983; Schaedel, 1951; Williams-Hunt, 1950). While visible light cameras were  
105 the first sensors used by archaeologists on aerial platforms, new instruments have expanded the  
106 ability of researchers to remotely sense landscapes using wavelengths across the electromagnetic  
107 spectrum. These new sensors can be passive – as in the case of multispectral cameras – or active  
108 – as in the case of light detecting and ranging (LiDAR) data.

109 LiDAR data are produced using a laser and sensor that records the return speeds of pulses  
110 of light that are reflected off of distant surfaces. LiDAR data often contain responses from  
111 multiple surfaces and can therefore provide information about feature elevations that are  
112 otherwise obscured by vegetative canopies. Consequently, LiDAR has proven to be particularly  
113 useful for detecting architectural structures (Eskew, 2008; Freeland et al., 2016; Johnson and  
114 Ouimet, 2014; Krasinski et al., 2016; Magnini et al., 2016; Prufer et al., 2015; Riley, 2009;  
115 Thompson and Prufer, 2015; Trier and Pilø, 2012; Trier and Zortea, 2012). Similar to the  
116 pioneering work in Guatemala (Canuto et al., 2018), there has been over a decade of productive  
117 studies using LiDAR that have taken place around the world (e.g., Inomata et al. 2018; Chase et  
118 al., 2014; Evans et al., 2013; Johnson and Ouimet, 2018; Wieshample et al., 2011; Witharana et  
119 al., 2018).

120 Two general classes of automated detection algorithms exist for analyzing remote sensing  
121 data: pixel- and object-based approaches. Pixel-based algorithms rely on spectral values encoded

122 in raster data. These approaches identify regions of data that match specific spectral values  
123 associated with targets of interest. Object-based image algorithms (OBIA), in contrast, use  
124 morphological characteristics such as texture, shape, and size – in addition to spectral values – to  
125 divide images into recognizable components with similar qualities. This feature of OBIA allows  
126 archaeologists to use attributes for identification that are often distinctive of cultural forms:  
127 shape, size, and spatial organization. With this ability, research over the past 15 years has  
128 demonstrated the potential of OBIA to efficiently identify anthropogenic structures from remote  
129 sensing data (e.g., De Laet et al., 2007; Larsen et al., 2008; Riley, 2009; Trier et al., 2015; Sevara  
130 et al., 2016; also see Davis, 2018 for a review of this literature).

## 131 *2.2 Segmentation*

132 Segmentation is a process that groups pixels into spectrally-similar segments. Software  
133 algorithms can then characterize these segments in terms of their geometric and textural  
134 properties. In the case of LiDAR data, these objects represent distinct topographic land forms on  
135 the ground. There are many forms of segmentation, but one of the most common processes used  
136 by archaeologists is multiresolution segmentation. Multiresolution segmentation adds to this  
137 process by iteratively dividing data into segments based on additional morphological differences  
138 such as shape, size, and texture (Magnini et al., 2016). For this reason, multiresolution  
139 segmentation provides greater ability to discriminate features of interest than segmentation  
140 methods that rely on just one set of criteria (Mao and Jing, 1992).

## 141 *2.3 Inverse Depression Analysis*

142 OBIA methods can focus on the use of hydrological depression algorithms (Lindsay and  
143 Creed, 2006; Wu et al., 2015, 2016) to identify archaeological mound features (Freeland et al.,

144 2016). This process requires the creation of an “inverse raster” in which a DEM is inverted so  
145 that mounds are represented as depressions. Freeland et al. (2016) has demonstrated this method  
146 in a study of a landscape in Tonga, revealing thousands of mounded features.

147 Stochastic depression analysis (SDA) is one algorithm that uses Monte Carlo simulation  
148 to map topographic depressions by evaluating morphological uncertainty (Lindsay and Creed,  
149 2006). The method works by estimating the likelihood that a given area contains an elevation  
150 change based on variability in topography. The benefit of SDA is that it highlights small  
151 elevation changes due to its sensitivity to topographic differences in elevation data. Here, we  
152 utilize an inversed version of SDA to identify mounded features in South Carolina. We initially  
153 process LiDAR data following Freeland et al. (2016) by creating an inversed DEM. We then  
154 apply an SDA algorithm and classify the results using morphological parameters such as  
155 compactness and mound size. This approach allows us to co-opt algorithms traditionally reserved  
156 for hydrological modeling for the detection of archaeological deposits.

#### 157 *2.4 Template Matching*

158 OBIA methods that employ template matching (TM) use statistical probabilities  
159 generated from aggregated examples of features that are characterized by pattern, texture, and  
160 shape. These probabilities form templates that are systematically and statistically used as  
161 comparisons to sub-sections of image data. Matches with templates are determined by  
162 identifying patterns in data that fall within specified statistical limits established by the template.

163 The archaeological utility of template matching is well-demonstrated (e.g., Kvamme,  
164 2013; Schneider et al., 2015; Trier et al., 2008, 2015; Trier and Zortea, 2012; Trier and Pilø,  
165 2012). One problem with template matching based approaches, however, is its tendency to

166 produce false positive and negative results. Reducing false positives requires careful  
167 construction of templates that narrowly define anthropogenic features. However, this step comes  
168 at the expense of an increased number of false negatives. The advantage of template matching,  
169 however, is that the statistical classifiers provide confidence intervals for detected objects,  
170 allowing one to quantitatively assess degrees of matching.

### 171 3.1 MATERIALS AND METHODS

172 In our evaluation of OBIA approaches for detecting mound features in heavily forested  
173 regions, we analyzed the same set of LiDAR data for each of the three study areas. These data  
174 come from the National Oceanic and Atmospheric Administration (NOAA)<sup>1</sup> and were created to  
175 plan for flood control and monitor coastal erosion. The raw data are available as processed  
176 Digital Elevation Models (DEMs) that have a spatial resolution of 1.2 meters, a resolution  
177 suitable for architecture-scaled feature analysis (see Beck et al., 2005). Using these data, we  
178 conducted analyses using (1) multiresolution segmentation, (2) Inverse Depression Analysis  
179 (IDA), (3) Template Matching (TM), and (4) a combined segmentation and TM approach. All of  
180 our analyses were conducted using a combination of eCognition (Trimble, 2016), WhiteBox  
181 GAT (Lindsay, 2016) and ArcGIS (ESRI, 2017).

#### 182 *3.1 Multiresolution Segmentation Analysis*

183 Following Magnini et al. (2016), we utilized a multiresolution segmentation process and  
184 selected segments of the LiDAR data that met circularity, asymmetry and compactness criteria  
185 stipulated by our summary of known features for the study area (Table 1). Asymmetry is

---

<sup>1</sup> <https://coast.noaa.gov/digitalcoast/data/coastallidar>

186 particularly effective for isolating archaeological features, as it is generally low in anthropogenic  
187 structures and high in naturally occurring landforms (Kvamme, 2013:55).

188 Table 1: Parameters used in multiresolution segmentation of the Beaufort County LiDAR data.

<i>Parameter</i>	<i>Threshold</i>
Area	$\leq 150 \text{ m}^2$
Circularity	$\geq 0.6$
Asymmetry	0 – 0.3
Compactness	$\geq 1.0$

189 To minimize false positive identifications, we compared the location of potential features  
190 with United States Geological Survey (USGS) land-use maps<sup>2</sup> and roadway shapefiles produced  
191 by the South Carolina Department of Transportation (DOT).<sup>3</sup> We eliminated those locations that  
192 appeared on “developed” or “disturbed” areas and within 10-meters of a roadway.<sup>4</sup> Next, we  
193 created a raster that represented the differences between local elevation and maximum  
194 neighborhood values calculated as focal statistics. Focal statistics help to highlight local  
195 elevation changes that would signify a mound feature. We then restricted our results to those  
196 features have a local positive elevation difference of half a meter or greater. Based on a review of  
197 known features in the area, topographic rises that are less than half-a-meter of relief are rarely  
198 associated with anthropogenic mounds or rings (Russo, 2006). Our process resulted in the  
199 identification of 2,490 potential features. Among these detections was a previously  
200 undocumented shell ring and earthen mound.

### 201 *3.2 Inverse Stochastic Depression Analysis (IDA)*

---

<sup>2</sup> Downloaded from the South Carolina Department of Natural Resources website (<http://www.dnr.sc.gov>)

<sup>3</sup> Downloaded from <http://www.gis.sc.gov/>

<sup>4</sup> We chose the buffer sizes based on standard road widths in the U.S.: 4-meters for single lane roads, 8-meters for two-lane, and 16-meters for 4-lane highways. For the buffers, we used 2 additional meters to serve as a buffer from the edges of the roads.

202 Here, we followed a strategy developed by Freeland et al. (2016) who demonstrated that  
203 depression analysis combined with morphometric criteria (size, shape, area, elevation and  
204 neighborhood) is effective in isolating mound structures. We created an inverse DEM using the  
205 equation

$$206 \quad \text{Inverse} = ((r - Z_{max}) \times (-1)) + Z_{min}$$

207 where  $r$  = DEM raster,  $Z_{max}$  = maximum elevation, and  $Z_{min}$  = minimum elevation. The results of  
208 the SDA analyses depend on the number of iterations that are used to process the data. In each  
209 iteration the assumption for topographic uncertainty is changed slightly to produce slightly  
210 different outcomes, and as the number of iterations increases, the algorithm produces more  
211 refined and consistent results. Using the SDA tool in Whitebox GAT (Lindsay, 2016) we  
212 compared the results of our analyses using 100, 200, and 300 iterations.<sup>5</sup> We filtered the result  
213 by then selecting only those features that were greater than 15m and less than 250m in diameter,  
214 the range known for rings and mounds in the region (Gibson, 1994; Russo, 2006; Walker, 2016).  
215 Finally, we excluded features that appeared on USGS land-use maps in areas that were  
216 designated as “disturbed”, “developed”, or “open water”, and those that were within 10-meters of  
217 a roadway and 20-meters of a major highway. This process produced 5,422 potential features.

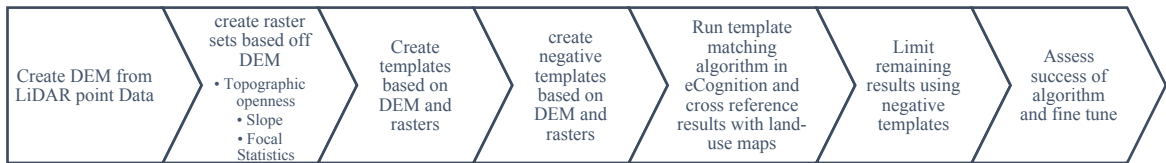
### 218 *3.3 Template Matching (TM)*

219 In our evaluation of template matching we followed steps in Figure 2. We created  
220 templates using a selection of 29 mound and ring features using characteristics of elevation,  
221 slope, focal statistics, and openness. Slope has been shown to be one of the most effective

---

<sup>5</sup> The number of iterations used for analysis impacts the amount of time required and depends on the processing capabilities of the computers used for data processing. Using 100 iterations for the analysis of our study areas required 36 hours. 1000 iterations would have taken at least a month of processing.

222 methods for identifying mound features as it shows a strong contrast between flat and uneven  
 223 surfaces, highlighting the outlines of mounds (e.g., Larson et al., 2017; Podobnikar, 2012; Prufer  
 224 et al., 2015; Riley, 2009; Thompson and Prufer, 2015). We used focal statistics to highlight  
 225 major changes in elevation that suggest the presence of topographic anomalies, similarly to the  
 226 processes mentioned above. Openness is a parameter that measures “topographic dominance” of  
 227 landforms (Yokoyama et al., 2002) and provides shade-free visualization for smaller topographic  
 228 anomalies.<sup>6</sup> Openness comes in two forms: positive and negative. Positive openness measures  
 229 the degree of concavity and negative openness measures the degree of convexity of a feature on a  
 230 landscape.



231  
 232 Figure 2: Steps involved in the use of template matching for the identification of mound features.  
 233

234 To create the templates, we used a sample of six known mound features that are recorded  
 235 in the South Carolina Archaeological Archives and 23 suspected features that were identified  
 236 manually using existing LiDAR data. These examples served as the basis for setting the  
 237 statistical limits for each of our templates.<sup>7</sup> Our use of multiple classes of data (elevation, slope,  
 238 openness, and focal statistics) to create templates enables us to compare results using different  
 239 characteristics. Following this process, we created 15 templates.<sup>8</sup>

---

<sup>6</sup> We calculated topographic openness using SAGA (Conrad et al., 2015)  
<sup>7</sup> The templates are available from the Open Repository at Binghamton University ([https://orb.binghamton.edu/anthro\\_data/3](https://orb.binghamton.edu/anthro_data/3))  
<sup>8</sup> We used the Template Editor tool in eCognition to create all of the templates

240 We also created 20 negative templates to represent those features that are topographically  
241 distinct but are not pre-contact mounds. Recent land disturbance, for example, might produce  
242 topographic features that could be confused as a prehistoric mound. To create these negative  
243 templates, we used 393 topographically distinct features that are not archaeological in their  
244 origin (e.g., linear contemporary features, building imprints, and river boundaries).

245 Once created, we used eCognition to apply the templates to the LiDAR data. This step  
246 produced over 10,000 potential identifications. Like the other two algorithms, we eliminated  
247 results that fell on land identified by USGS land-use maps as “developed” or “disturbed”, those  
248 that were located within waterbodies, and those that fell within 10-meters of roadways and 20  
249 meters of major highways. We also rejected all results that the algorithm calculated as at least  
250 75% likely to be a false positive based on their similarity to our negative templates. The final  
251 results included only those detections that were calculated by the algorithm to be at least 60%  
252 “most statistically likely.” The final template matching process produced 10 potential features.

### 253 *3.4: Combined TM and Segmentation Method*

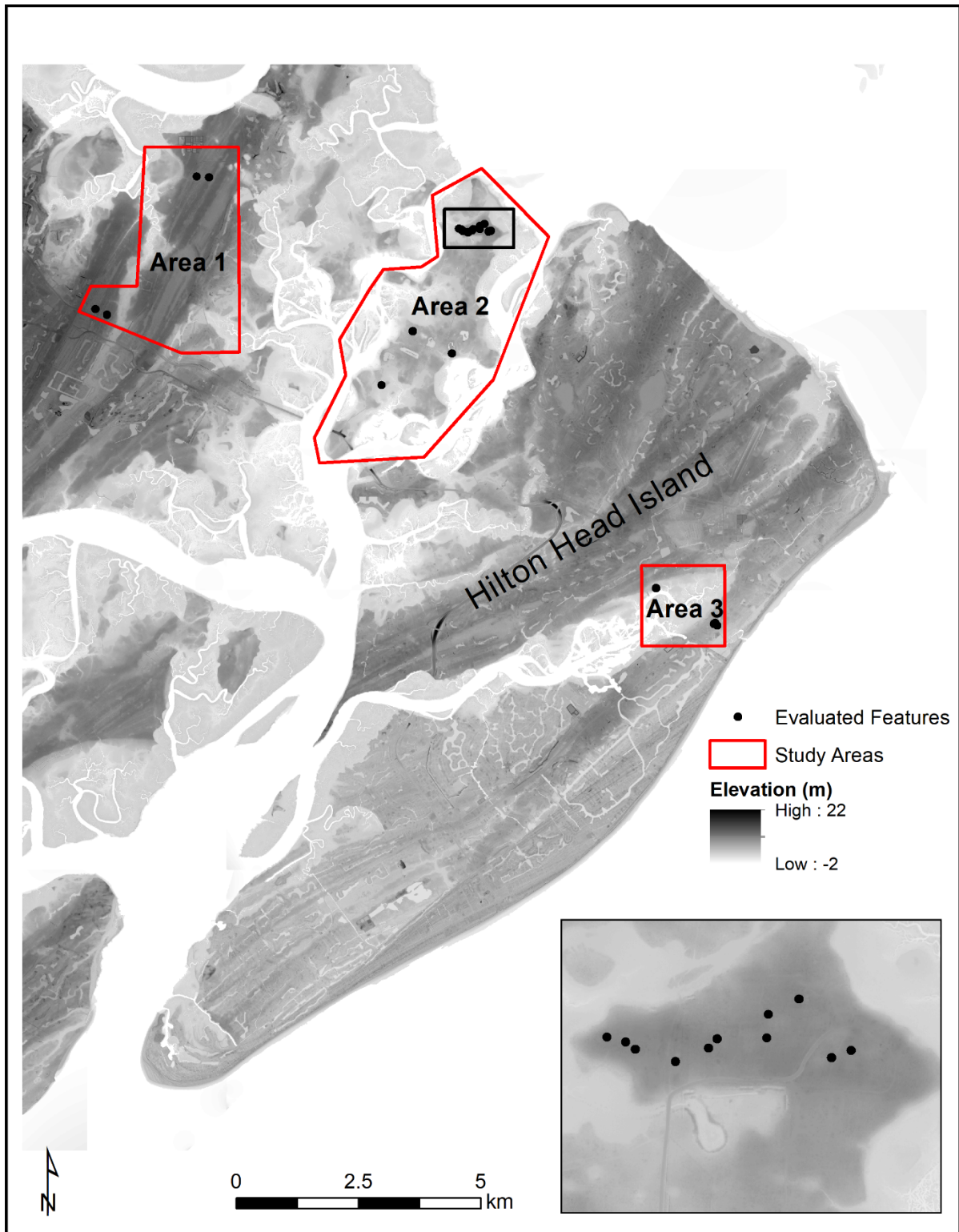
254 In order to evaluate the degree to which the strengths of each OBIA method can be  
255 combined to produce superior results, we also developed a multidimensional algorithm that  
256 includes segmentation and template matching steps (see Davis et al., 2018). This algorithm  
257 begins with template matching to create correlation-coefficient maps of potential features. Then,  
258 we used multiresolution segmentation on these results. We subsequently isolated those features  
259 that had a local elevation difference of between 0.5 and 5 meters from the surrounding area  
260 (Russo, 2006). We calculated neighborhood changes in elevation using the focal statistics tool  
261 (shape = circle, height and width = 5) in ArcMap 10.5 (ESRI 2017). We rejected all results that

262 occur on developed land, that are located in areas close to roadways, and that have slopes that are  
263 less than five or greater than 50 degrees.

264         Next, we superimposed the remaining results with the correlation rasters that we  
265 produced during the template matching process. As the templates are used to iteratively scan  
266 sections of the LiDAR data, each section examined is assigned a positive and negative  
267 correlation coefficient value that corresponds to the overall match of a location to the positive  
268 and negative templates. We used the negative correlation raster to eliminate results that were  
269 identified as at least 75% likely to be false positives. Lastly, we created a new raster by  
270 subtracting the negative correlation coefficient from the positive correlation coefficient. Areas of  
271 this raster containing negative values indicate strong likelihoods of false identifications, as they  
272 closely correlate with non-mound features in the negative template. As such, we rejected any  
273 results that overlap a portion of this raster containing negative values. This process left 10  
274 potential features.

### 275 *3.5 Ground Survey*

276         Following our OBIA analyses, we chose 22 locations to visit on the ground to evaluate  
277 the degree to which the algorithmic detection correctly identified anthropogenic features (Figure  
278 3). All of these features are located on public land and were accessible for pedestrian survey.



279  
 280  
 281  
 282

Figure 3: Features evaluated during ground surveys. The inset provides detail of an area of Study Area 2 (marked by the black box) where a number of features were found in close proximity (Color online).

283 4.1 RESULTS

284 The results of each OBIA analysis shows that there are distinct differences in the yield of  
 285 potential features depending on the approach used (Tables 2 and 3). Areas 1 and 2 (see Figure 1)  
 286 provide useful environments within which to test each OBIA method. Within Area 2, the  
 287 combined method did not identify any features, indicating that it cannot identify midden  
 288 structures effectively, as many archaeological middens are present on Pinckney Island (Charles,  
 289 1984; Kanaski, 1997; Trinkley, 1981). Area 3 (Figure 1) encompasses publicly available land on  
 290 Hilton Head Island, some of which is highly developed. The number of features identified is  
 291 substantial given its small size (~3 km<sup>2</sup>) and indicates a high level of false positive  
 292 identifications in developed locations. The template matching and combined approaches only  
 293 identify a handful of potential sites, suggesting their capability of reducing false identifications.

294 Table 2: Total detections made by each OBIA technique.

OBIA Method	Total Detections	Total Detections	Total Detections
	Study Area 1	Study Area 2	Study Area 3
Segmentation	1,399	1,091	380
IDA (100 iterations)	3,332	1,677	413
IDA (200 iterations)	1,582	1,829	807
IDA (300 iterations)	1,093	2,485	817
Template Matching	6	3	3
Combined	7	0	3

295

296 The segmentation approach was particularly effective in identifying mounds, yet also  
 297 produced many results that are likely false positives (Figure 4). Using shapefiles provided by the

298 South Carolina SHPO, we determined that 384 detections made by segmentation are located on  
 299 84 previously surveyed archaeological sites on Pinckney Island (Supplemental Table 1).  
 300 Significantly, the segmentation analysis identified a new mound feature that is previously  
 301 unrecorded (this feature was also identified by TM and IDA but was missed by the combined  
 302 method).

303 Table 3: OBIA Method Results from Field Survey

304

OBIA Method	Sites Surveyed	Accurate identifications determined by field survey	False Positives determined by field survey	Rate of positive identification/false positives based on field survey	Total Detections in Study Areas	Potential new mound features
Segmentation Classification	12	6	6*	1:1	2,490	1,245
IDA (100 iterations)	14	5	9**	5:9	5,422	3,012
TM	6	3	3	1:1	10	5
Combined (segmentation and TM)	4	4	0	1:0	10	10

\* Two sites were inconclusive  
 \*\* One site was inconclusive

305 IDA proved successful in identifying pre-contact mounds, including shell rings (Figure  
 306 5). Nonetheless, a common issue with this method is the plethora of false positive results that  
 307 occur due to natural topographic changes. Some of the limitations of IDA in feature detection,  
 308 however, are likely due to resolution limits of the LiDAR DEM that we used, and the number of  
 309 iterations performed on the analysis. Using higher-resolution LiDAR as well as greater  
 310 processing hardware may improve the relative effectiveness of IDA in detecting features.

311 To evaluate the degree to which the amount of processing can improve our results, we  
 312 conducted our IDA analyses with 200, and 300 iterations. In all instances, the increase in  
 313 iterations correlates with an improvement in archaeological feature detection (Tables 4 and 5). In

314 all three study areas, false positive results identified using 100 iterations and surveyed were not  
 315 reidentified using 300 iterations (Table 5).

316 Looking at Area 2 (Pinckney Island), we compared identified results to known  
 317 archaeological sites in this area in order to gauge the accuracy of IDA in identifying previously  
 318 detected archaeological deposits (Table 4; also see Supplemental Table 1). We chose this area  
 319 because of its history of extensive archaeological surveys. In addition to increased iterations, it is  
 320 possible that with higher resolution DEMs better discrimination of topographic features can be  
 321 obtained (Vaze et al., 2010).

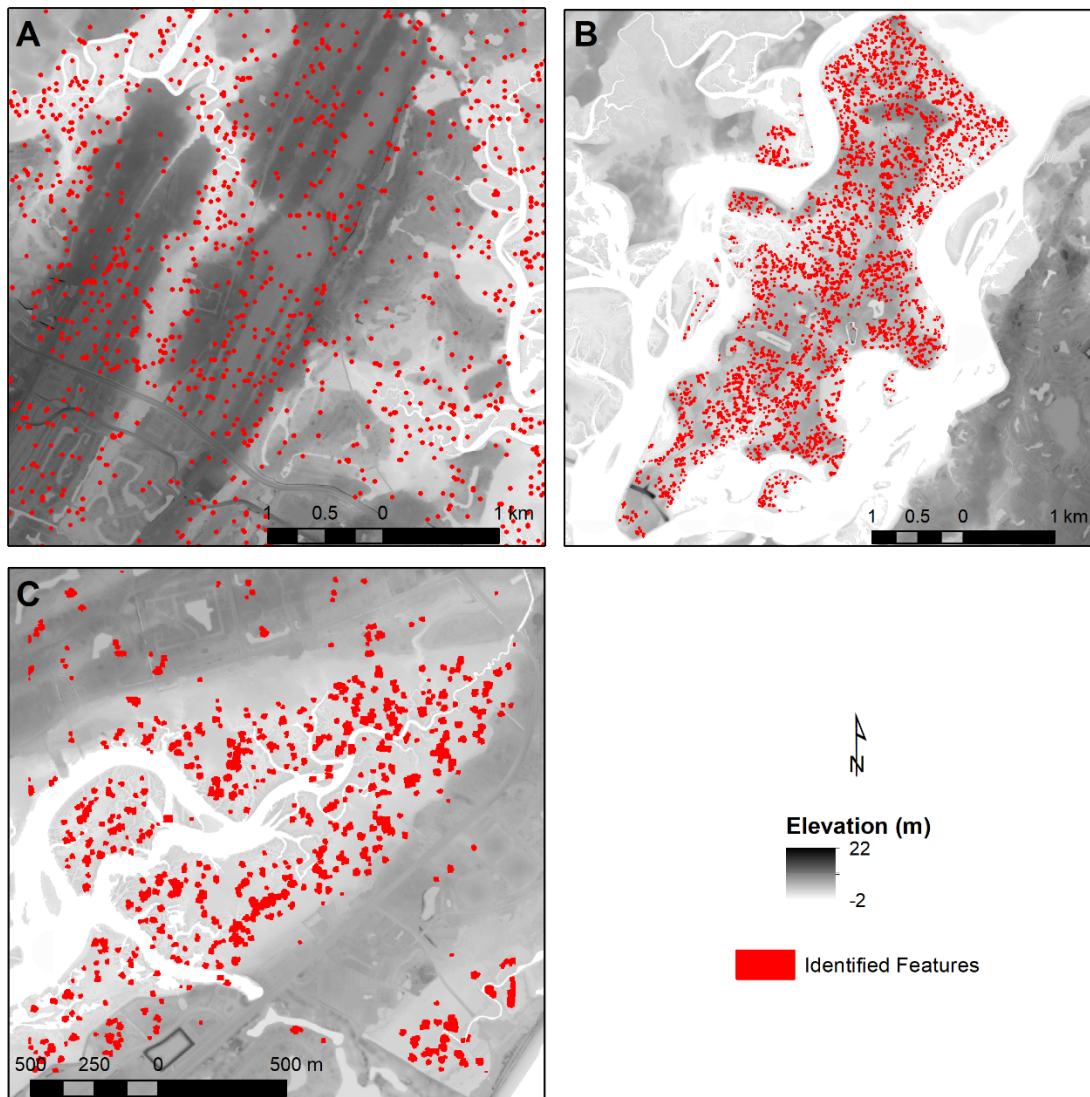
322 Table 4: Change in detection accuracy for known archaeological deposits in Area 2 using  
 323 increasing numbers of iterations. As the number of iterations increases, so too does the number  
 324 of identified archaeological deposits.

<b>Number of Iterations</b>	<b>Number of Identified Archaeological Deposits</b>
<b>100</b>	40
<b>200</b>	59
<b>300</b>	60

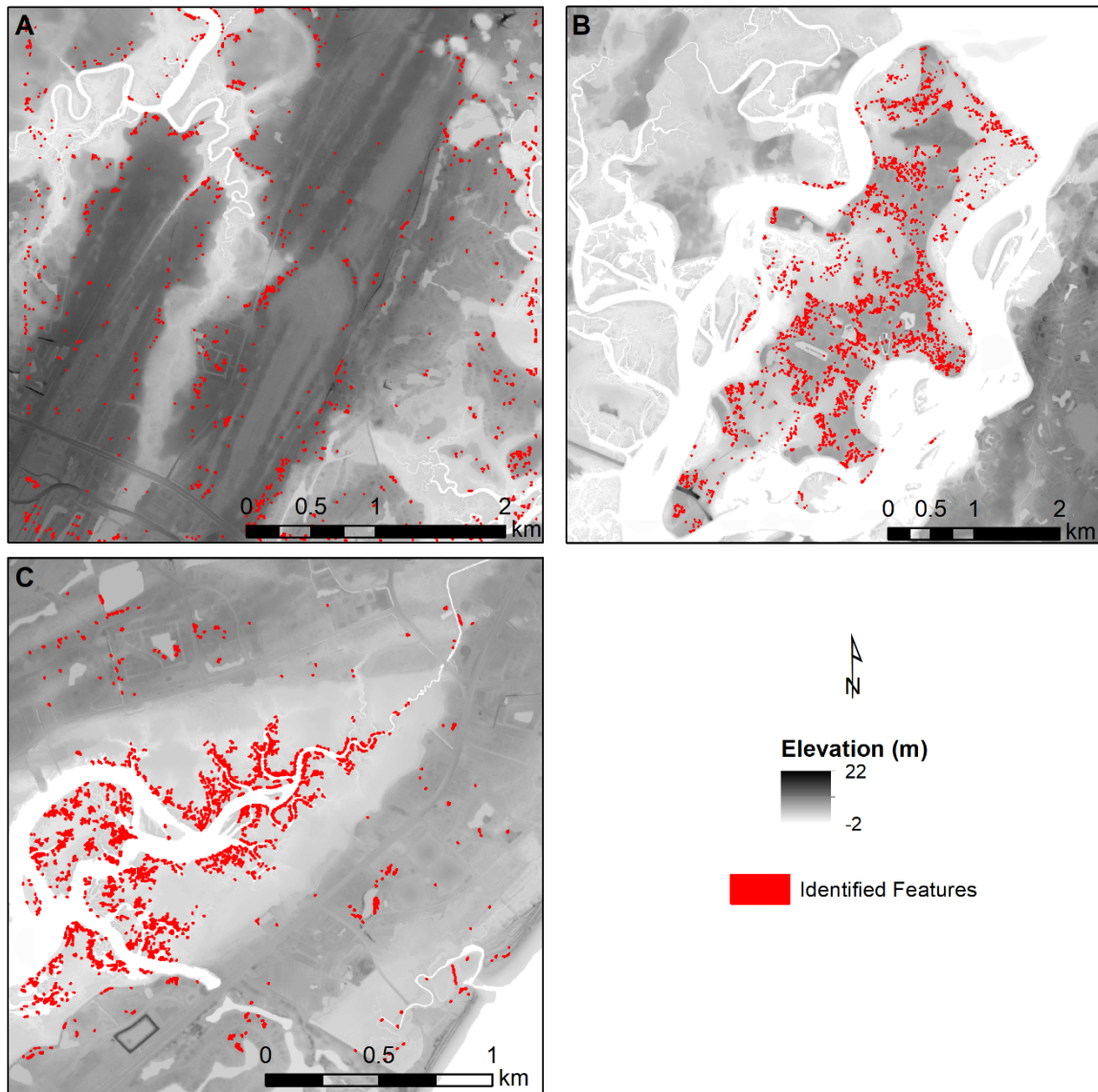
325 Table 5: Overall accuracy for IDA using increasing numbers of iterations. As the number of  
 326 iterations increases, the number of false positive detections decreases, and the overall accuracy  
 327 increases.

<b>Number of Iterations</b>	<b>True Positive Identifications (Determined by ground-survey)</b>	<b>False Positive Identifications (Determined by ground-survey)</b>	<b>Total Detections</b>	<b>Overall Accuracy</b>
<b>100</b>	5	9	5,422	35.71%
<b>200</b>	3	3	4,218	50.00%
<b>300</b>	5	2	4,395	71.43%

328



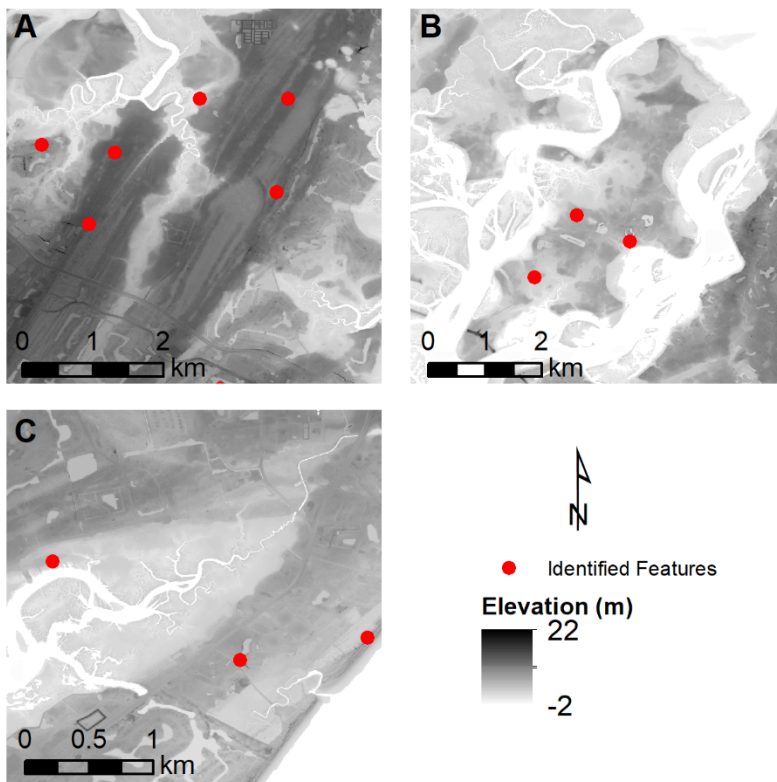
329  
 330 Figure 4: Segmentation results. A: Study Area 1 results. The majority of the identifications are  
 331 false positives caused by natural phenomena. B: Study Area 2 results. C: Study Area 3 results.  
 332 The majority of identifications are explained as natural levee features that line the bayous.  
 333 Several other identifications in this scene are housing footprints or other recent landscape  
 334 disturbances. Highly developed areas tend to show numerous false positive results (Color  
 335 online).



336  
 337 Figure 5: Results of IDA analysis using 300 iterations. A: Study Area 1 results. In addition to  
 338 several mounds, IDA also identified a new shell ring site in this area. B: Study Area 2 results. C:  
 339 Study Area 3 results. Many results in all areas are the result of natural topographic changes  
 340 and/or modern disturbance (Color online).

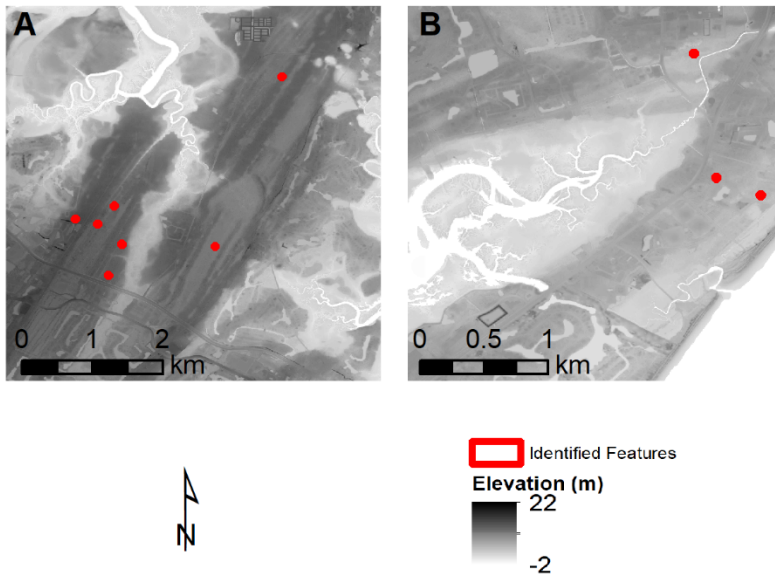
341 In contrast to segmentation and IDA, template matching *only* identified features that were  
 342 anthropogenic in origin, though the method missed a shell-ring that was located by segmentation  
 343 (Figures 6). Finally, our combined approach that includes template matching and segmentation  
 344 improved on all of these results by retaining only the positively identified features (see Figure 7).

345



346

347 Figure 6: Results of the template matching algorithm on the three study areas. A: Study Area 1  
 348 results. The algorithm failed to identify the shell ring site (indicated by arrow). B: Study Area 2  
 349 results. All identified locations are anthropogenic. Two of the three have archaeological contexts.  
 350 C: Study Area 3 results. Two of the three features were surveyed and were both anthropogenic.  
 351 Neither one was archaeological in context. White areas represent water and coastline (Color  
 352 online).



353  
 354 Figure 7: Results of the combined segmentation and template matching algorithm. A: Study Area  
 355 1 results. B: Study Area 3 results. In comparison to the segmentation and IDA methods (see  
 356 Figures 4 and 5) the combined method provides fewer false positives (Color online).

357 *4.4 Method Results and Comparisons*

358 Study Area 3 proved to be problematic for the detection of archaeological deposits due to  
 359 the extensive recent land disturbance activity. In general, any use of automated techniques such  
 360 as OBIA is going to be hampered in areas that have been subject to development. One can expect  
 361 considerably more manual labor will be required to filter false positives from total results. The  
 362 combined approach, however, was the most effective in these conditions and did not falsely  
 363 identify the hundreds of features that were identified by the other methods (Figure 7). This result  
 364 further emphasizes the benefits of using a combined approach for archaeological prospection.

365 Numerically, segmentation and IDA were the most successful OBIA methods for  
 366 identifying mounded features, as they detected the most archaeological sites compared to the  
 367 other methods (Table 2). They yield, however, the highest number of false positives. Using a  
 368 greater number of iterations appears to alleviate this issue and makes IDA far more successful

369 than a pure segmentation procedure. The use of template matching produced no false positives  
 370 related to natural phenomena but failed to discriminate between prehistoric and historic features.  
 371 Our new combined approach that includes template matching and segmentation provided the  
 372 greatest consistency in correctly identifying archaeological features (also see Davis et al., 2018)  
 373 (Table 6).

374 Table 6: Archaeological utility of OBIA methods. Topographic discrimination refers to each  
 375 method’s ability to distinguish between natural and anthropogenic features. Archaeological  
 376 detection accuracy refers to the ratio of positive detections to false ones. Overall utility is the  
 377 average of the topographic discrimination and archaeological detection accuracies.

METHOD	Segmentation	IDA (100 iterations)	IDA (200 iterations)	IDA (300 iterations)	TM	Combined
Topographic Discrimination Accuracy	50%	57.14%	66.67%	85.71%	100%	100%
Archaeological Detection Accuracy	50%	35.71%	50%	71.43%	50%	100%
Overall Utility (average of accuracies)	<b>50%</b>	<b>46.43%</b>	<b>58.34%</b>	<b>78.57%</b>	<b>75%</b>	<b>100%</b>

378 5.1 DISCUSSION AND CONCLUSION

379 While each OBIA method that we evaluated yields positive identifications, our results  
 380 show that a combination of approaches produces the most reliable information for archaeological  
 381 prospection. Of course, some of the differences we note in our analyses depend on the quality of  
 382 the data we used: the effectiveness of methods depends to some degree on the resolution and  
 383 quality of the data. The difference between segmentation and IDA in our study of Beaufort  
 384 County, for example, was likely due to the limits of the resolution of our LiDAR data. Improved  
 385 resolution of the LiDAR data will address the deficiency observed in this study. By tripling the  
 386 number of iterations, IDA yielded more accurate results than segmentation, as opposed to  
 387 slightly less accurate results using only 100 iterations. The processing requirements, however,

388 make IDA less useful for large-scale landscape studies, as the amount of computing power  
389 required makes the process extremely time consuming.

390         The results here are promising but it should be noted that a single universal algorithm is  
391 unlikely to be developed. In the case of OBIA, the analyst must always establish the definition  
392 for classes of objects to be identified in advance. These definitions must be based on specific  
393 hypotheses about the necessary and sufficient conditions needed for the algorithm to identify a  
394 feature of interest. The parameters for these conditions can be derived using regionally-specific  
395 parameters, but doing so means that the conditions will be contingency-bound generalizations  
396 and will be incapable of detecting previously unknown features with morphologies other than  
397 those described in reference samples. For this reason, analyses must be repeated by varying the  
398 parameters to test new hypotheses and as new knowledge of the local archaeological is  
399 developed.

400         Ultimately, the identification of new aspects of the archaeological record in the American  
401 Southeast will permit for researchers to re-evaluate our current notions about pre-contact  
402 settlement patterns, as well as the significance of features like shell rings. The shell ring  
403 identified by this study (also see Davis et al., 2018) is significantly smaller than most known  
404 shell rings in this area. The methods and datasets used here permit for the detection of features as  
405 small as a few meters across and about half-a-meter tall. The average diameter of known ring  
406 plazas in South Carolina is 32 meters (Russo 2006:25). The ring discovered here has a plaza  
407 diameter of approximately 16 meters, half that of the size of known rings. Additionally, the  
408 maximum diameter of the ring is only 36 meters. Compared to the average in South Carolina of  
409 64 meters (Russo 2006:25), this ring is considerably smaller than those previously studied. As  
410 such, new discoveries may reveal new information about the range of feature structure and

411 composition, challenging previous notions of prehistoric activity (e.g., Russo, 2004; Saunders,  
412 2004; Trinkley, 1985).

413         This substantial difference in size of this new ring feature compared to previously  
414 surveyed rings in this area also speaks to a bias in archaeological knowledge towards  
415 monumental structures compared to smaller ones. This requires high resolution datasets, as the  
416 higher the spatial resolution, the smaller the objects that are detectable. A future avenue of  
417 research must focus on the potential for remote sensing surveys in alleviating human error in  
418 traditional surveying, where visibility becomes a considerable issue in detection in heavily  
419 vegetated environments (Hirth 1978; Nance 1979; Schiffer et al. 1978).

420         The results of our new approach show several new features that were undetected by  
421 previous manual surveys (see Davis et al., 2018). These features include previously unrecorded  
422 deposits such the new shell ring in Study Area 1 and a pre-contact mound in Study Area 2. As  
423 such, the use of automated methods is successful in picking out features that manual approaches  
424 overlook, and ensures full, systematic coverage of areas being surveyed. Nevertheless, it should  
425 be stressed that manual evaluation is also an essential step in analyzing remote sensing data, as it  
426 often provides the first step in building robust datasets that can be used as training data for more  
427 complex automated methods.

428         Urbanization and climate related sea level changes pose imminent threats to cultural  
429 resources in areas such as Beaufort County, but also across the American Southeast. The use of  
430 remote sensing technologies such as LiDAR and computational algorithms offer new means for  
431 addressing existing deficiencies in our knowledge of the archaeological record. While no single  
432 algorithm offers a universal solution, the use of LiDAR data and OBIA can yield accurate  
433 identifications of mound features that lay under tree canopies and across large areas. While

434 preliminary, this study demonstrates the potential for OBIA and remote sensing to greatly assist  
435 in archaeological landscape survey efforts. Given the urgency to document our extant  
436 archaeological record before it is lost, such an approach promises to greatly contribute to our  
437 knowledge of the archaeological record.

438

#### 439 ACKNOWLEDGEMENTS

440 The authors would like to thank the reviewers for their helpful comments on the manuscript. All  
441 related datasets are available through the Open Repository at Binghamton University  
442 ([https://orb.binghamton.edu/anthro\\_data/4/](https://orb.binghamton.edu/anthro_data/4/)).

443 FUNDING: This work was supported by the National Geographic Grant Reward Number HJ-  
444 107R-17; and Binghamton University.

#### 445 6.1 REFERENCES

446

447 Agache, R., 1968. Essai d'utilisation aérienne et au sol d'émulsions spectrozonales, dites  
448 infrarouges couleurs. *Society Préhistorique de France* 65, 198–201.

449 Anderson, D.G., 2012. Monumentality in eastern North America during the Mississippian  
450 period, in: Burger, R.L., Rosenwig, R.M. (Eds.), *Early New World Monumentality*.  
451 University Press of Florida, Gainesville, pp. 78–108.

452 Anderson, D.G., 2004. Archaic Mounds and the Archaeology of Southeastern Tribal Societies,  
453 in: Gibson, J.L., Carr, P.J. (Eds.), *Signs of Power: The Rise of Cultural Complexity in the*  
454 *Southeast*. University of Alabama Press, Tuscaloosa, pp. 270–299.

455 Anderson, D.G., Bissett, T.G., Yerka, S.J., Wells, J.J., Kansa, E.C., Kansa, S.W., Myers, K.N.,  
456 DeMuth, R.C., White, D.A., 2017. Sea-level rise and archaeological site destruction: An  
457 example from the southeastern United States using DINAA (Digital Index of North

458 American Archaeology). PLOS ONE 12, e0188142.  
 459 <https://doi.org/10.1371/journal.pone.0188142>

460 Banning, E.B., Hawkins, A.L., Stewart, S.T., Hitchings, P., Edwards, S., 2017. Quality  
 461 Assurance in Archaeological Survey. *J. Archaeol. Method and Theory* 24, 466–488.  
 462 <https://doi.org/10.1007/s10816-016-9274-2>

463 Beck, A., Philip, G., Abdulkarim, M., Donoghue, D., 2007. Evaluation of Corona and Ikonos  
 464 high resolution satellite imagery for archaeological prospection in western Syria. *Antiquity*  
 465 81, 161–175. <https://doi.org/10.1017/S0003598X00094916>

466 Becker, P.W., 1975. Pattern recognition applications in work with ancient objects, in: Proc.  
 467 NATO Advanced Study Institute on Pattern Recognition—Theory and Applications, Sept.  
 468 8-17.

469 Bintliff, J., Howard, P., Snodgrass, A., 1999. The Hidden Landscape of Prehistoric Greece. *J.*  
 470 *Mediterr. Archaeol.* 12, 139–168.

471 Bintliff, J.L., 2000. The concepts of “site” and “off site” archaeology in surface artefact survey,  
 472 in: Pasquinucci, M., Tremont, F. (Eds.), *Non-Destructive Techniques Applied to Landscape*  
 473 *Archaeology*. Oxbow Books, Oxford, pp. 200–215.

474 Bradford, J.S.P., 1956. Mapping Two Thousand Tombs from the Air: How Aerial Photography  
 475 Plays its Part in Solving the Riddle of the Etruscans. *Illustrated London News*, London.

476 Buettner-Januch, J., 1954. Use of infrared photography in archaeological work. *Am. Antiq.* 20,  
 477 84–87.

478 Caldwell, J.R., 1952. The Archeology of Eastern Georgia and South Carolina, in: Griffin, J.B.  
 479 (Ed.), *Archeology of Eastern United States*. University of Chicago Press, Chicago, pp. 312–  
 480 321.

481 Calmes, A.R., 1967. Test excavations at two Late Archaic sites on Hilton Head Island. Presented  
 482 at the Southeastern Archaeological Conference, Macon, GA.

483 Campbell, K.M., 1981. Remote Sensing: Conventional and Infrared Imagery for Archaeologists.  
 484 *University of Calgary Archaeology Association* 11, 1–8.

485 Canuto, M.A., Estrada-Belli, F., Garrison, T.G., Houston, S.D., Acuña, M.J., Kováč, M.,  
 486 Marken, D., Nondédéo, P., Auld-Thomas, L., Castanet, C., Chatelain, D., Chiriboga, C.R.,  
 487 Drápela, T., Lieskovský, T., Tokovinine, A., Velasquez, A., Fernández-Díaz, J.C., Shrestha,

488 R., 2018. Ancient lowland Maya complexity as revealed by airborne laser scanning of  
489 northern Guatemala. *Science* 361, eaau0137. <https://doi.org/10.1126/science.aau0137>

490 Capper, J.E., 1907. Photographs of Stonehenge as seen from a war balloon. *Archaeologia* 60,  
491 571.

492 Charles, F.N., 1984. *Archaeology at Last End Point: The Testing and Evaluation of Three Shell*  
493 *Midden Sites (38BU66, 38BU166; and 38BU167) at the Pinckney Island National Wildlife*  
494 *Refuge*. Southwind Archaeological Enterprises, Tallahassee.

495 Chase, A.S.Z., Chase, D.Z., Chase, A.F., 2017. LiDAR for Archaeological Research and the  
496 Study of Historical Landscapes, in: Masini, N., Soldovieri, F. (Eds.), *Sensing the Past*.  
497 Springer International Publishing, Cham, pp. 89–100. [https://doi.org/10.1007/978-3-319-](https://doi.org/10.1007/978-3-319-50518-3_4)  
498 [50518-3\\_4](https://doi.org/10.1007/978-3-319-50518-3_4)

499 Chase, A.F., Chase, D.Z., Awe, J.J., Weishampel, J.F., Iannone, G., Moyes, H., Yaeger, J.,  
500 Kathryn Brown, M., 2014. The Use of LiDAR in Understanding the Ancient Maya  
501 Landscape. *Adv. Archaeol. Pract.* 2, 208–221. <https://doi.org/10.7183/2326-3768.2.3.208>

502 Claassen, C., 2010. *Feasting with Shellfish in the Southern Ohio Valley: Archaic Sacred Sites*  
503 *and Rituals*. University of Tennessee Press, Knoxville.

504 Claassen, C., 2008. Shell Symbolism in Pre-Columbian North America, in: Andrzej, A., Roberto,  
505 C. (Eds.), *Early Human Impact on Megamolluscs*. Archaeopress, Oxford, pp. 37–43.

506 Claassen, C., 1991. Normative Thinking and Shell-Bearing Sites. *Archaeolog. Method and*  
507 *Theory* 3, 249–298.

508 Claassen, C., 1986. Shellfishing Seasons in the Prehistoric Southeastern United States. *Am.*  
509 *Antiq.* 51, 21–37.

510 Claflin, W.H., 1931. *The Stalling’s Island Mound, Columbia County, Georgia*, Papers of the  
511 Peabody Museum of American Archaeology and Ethnology, Harvard University.  
512 Cambridge.

513 Conrad, O., Bechtel, B., Bock, M., Dietrich, H., Fischer, E., Gerlitz, L., Wehberg, J., Wichmann,  
514 V., Böhner, J., 2015. System for Automated Geoscientific Analyses (SAGA) v. 2.1.4.  
515 *Geosci. Model Dev.* 8, 1991–2007. <https://doi.org/10.5194/gmd-8-1991-2015>

516 Crusoe, D.L., DePratter, C.B., 1976. New Look at the Georgia Coastal Shell Mound Archaic.  
517 *Fla. Anthropol.* 29, 1–23.

518 Davis, D.S., 2018. Object-based image analysis: a review of developments and future directions  
519 of automated feature detection in landscape archaeology. *Archaeological Prospection*. In  
520 Press. <https://doi.org/10.1002/arp.1730>

521 Davis, D.S., Sanger, M.C., Lipo, C.P., 2018 Automated mound detection using LiDAR survey in  
522 Beaufort County, SC. *Southeastern Archaeology*. 1-15,  
523 <https://doi.org/10.1080/0734578X.2018.1482186>.

524 De Laet, V., Paulissen, E., Waelkens, M., 2007. Methods for the extraction of archaeological  
525 features from very high-resolution Ikonos-2 remote sensing imagery, Hisar (southwest  
526 Turkey). *J. Archaeol. Sci.* 34, 830–841. <https://doi.org/10.1016/j.jas.2006.09.013>

527 Drager, D.L., 1983. Projecting archaeological site concentrations in the San Juan Basin, New  
528 Mexico, in: Drager, D.L., Lyons, T.R. (Eds.), *Remote Sensing in Cultural Resource*  
529 *Management*. National Park Service, Washington D. C.

530 Engelbach, R., 1929. The aeroplane and Egyptian archaeology. *Antiquity* 3, 47–73.

531 Eskew, K., 2008. Using LiDAR and GIS to Detect Prehistoric Earthworks in the Yazoo Basin,  
532 Mississippi (MA Thesis). Department of Anthropology, California State University, Long  
533 Beach.

534 ESRI, 2017. ArcGIS Version 10.5. Redlands, CA: Environmental Systems Research Institute,  
535 Inc.

536 Evans, D.H., Fletcher, R.J., Pottier, C., Chevance, J.-B., Soutif, D., Tan, B.S., Im, S., Ea, D., Tin,  
537 T., Kim, S., Cromarty, C., De Greef, S., Hanus, K., Baty, P., Kuszinger, R., Shimoda, I.,  
538 Boornazian, G., 2013. Uncovering archaeological landscapes at Angkor using lidar. *Proc.*  
539 *Natl. Acad. Sci.* 110, 12595–12600. <https://doi.org/10.1073/pnas.1306539110>

540 Fairbanks, C.H., 1942. The Taxonomic Position of Stalling's Island, Georgia. *Am. Antiq.* 7,  
541 223–231.

542 Ford, J.A., Willey, G.R., 1941. An Interpretation of the Prehistory of the Eastern United States.  
543 *Am. Anthropol.* 43, 325–363.

544 Freeland, T., Heung, B., Burley, D.V., Clark, G., Knudby, A., 2016. Automated feature  
545 extraction for prospection and analysis of monumental earthworks from aerial LiDAR in the  
546 Kingdom of Tonga. *J. Archaeol. Sci.* 69, 64–74. <https://doi.org/10.1016/j.jas.2016.04.011>

547 Frierson, J.L., 2000. South Carolina Prehistoric Earthen Indian Mounds (Master's Thesis).  
548 University of South Carolina, Columbia.

549 Harp, E.J., 1966. Anthropology and remote sensing. Office of Aerospace Research, Air Force  
550 Cambridge Research Laboratories, Terrestrial Sciences Laboratory, Bedford, Mass.

551 Hirth, K.G., 1978. Problems in Data Recovery and Measurement in Settlement Archaeology.  
552 *J. Field Archaeol.* 5, 125–131. <https://doi.org/10.1179/009346978791489871>

553 House, J.H., Ballinger, D.L., 1976. An Archeological Survey of the Interstate 77 Route in the  
554 South Carolina Piedmont (No. 143), Research Manuscript Series. The South Carolina  
555 Institute of Archeology and Anthropology--University of South Carolina.

556 Howe, L., 2014. Embodied Tribalography: Mound Building, Ball Games, and Native Endurance  
557 in the Southeast. *Stud. Am. Indian Lit.* 26, 75–93.

558 Inomata, T., Pinzón, F., Ranchos, J.L., Haraguchi, T., Nasu, H., Fernandez-Diaz, J.C., Aoyama,  
559 K., Yonenobu, H., 2017. Archaeological Application of Airborne LiDAR with Object-  
560 Based Vegetation Classification and Visualization Techniques at the Lowland Maya Site of  
561 Ceibal, Guatemala. *Remote Sens.* 9, 563. <https://doi.org/10.3390/rs9060563>

562 Inomata, T., Triadan, D., Pinzón, F., Burham, M., Ranchos, J.L., Aoyama, K., Haraguchi, T.,  
563 2018. Archaeological application of airborne LiDAR to examine social changes in the  
564 Ceibal region of the Maya lowlands. *PLOS ONE* 13, e0191619.  
565 <https://doi.org/10.1371/journal.pone.0191619>

566 Jensen, J.R., 2007. Remote Sensing of the Environment: An Earth Resource Perspective, 2nd ed.  
567 Pearson Prentice Hall, Upper Saddle River, NJ.

568 Johnson, K.M., Ouimet, W.B., 2018. An observational and theoretical framework for interpreting  
569 the landscape palimpsest through airborne LiDAR. *Appl. Geograph.* 91, 32–44.  
570 <https://doi.org/10.1016/j.apgeog.2017.12.018>

571 Johnson, K.M., Ouimet, W.B., 2014. Rediscovering the lost archaeological landscape of southern  
572 New England using airborne light detection and ranging (LiDAR). *J. Archaeol. Sci.* 43, 9–  
573 20. <https://doi.org/10.1016/j.jas.2013.12.004>

574 Jones, W.B., Brannon, P.A., Hough, W., Bunnell, C.E., Mason, J.A., Stirling, M.W., Cummings,  
575 B., Halseth, O.S., Gladwin, H.S., Colton, H.S., Morris, E.H., 1933. Archaeological Field  
576 Work in North America during 1932. *Am. Anthropol.* 35, 483–511.

577 Kanaski, R.S., 1997. Archaeological Assessment and Survey of Proposed Pond Expansions,  
578 Boardwalk, and Erosion Control at Shell Point, Pinckney Island National Wildlife Refuge,  
579 Beaufort County, South Carolina. U.S. Fish and Wildlife Services.

580 Krasinski, K.E., Wygal, B.T., Wells, J., Martin, R.L., Seager-Boss, F., 2016. Detecting Late  
581 Holocene cultural landscape modifications using LiDAR imagery in the Boreal Forest,  
582 Susitna Valley, Southcentral Alaska. *J. Field Archaeol.* 41, 255–270.  
583 <https://doi.org/10.1080/00934690.2016.1174764>

584 Kvamme, K., 2013. An Examination of Automated Archaeological Feature Recognition in  
585 Remotely Sensed Imagery, in: Bevan, A., Lake, M. (Eds.), *Computational Approaches to*  
586 *Archaeological Spaces*. Left Coast Press, Walnut Creek, pp. 53–68.

587 Larsen, S.Ø., Trier, Ø.D., Solberg, R., 2008. Detection of ring shaped structures in agricultural  
588 land using high resolution satellite images, in: *Pixels, Objects, Intelligence: Geographic*  
589 *Object-Based Image Analysis for the 21st Century*. Presented at the GEOBIA, Calgary,  
590 Alberta, Canada.

591 Lindbergh, C.A., 1929a. Colonel and Mrs. Lindbergh aid archaeologists, Carnegie Institute  
592 Reports. Carnegie Institute, New York.

593 Lindbergh, C.A., 1929b. The discovery of the ruined Maya cities. *Sci.* 70, 12–13.

594 Lindsay, J.B., 2016. Whitebox GAT: A case study in geomorphometric analysis. *Comput. &*  
595 *Geosci.* 95, 75–84. <https://doi.org/10.1016/j.cageo.2016.07.003>

596 Lindsay, J.B., Creed, I.F., 2006. Distinguishing actual and artefact depressions in digital  
597 elevation data. *Comput. & Geosci.* 32, 1192–1204.  
598 <https://doi.org/10.1016/j.cageo.2005.11.002>

599 Lyman, R.L., O'Brien, M.J., Dunnell, R.C., 1997. *The Rise and Fall of Culture History*. Plenum  
600 Press, New York.

601 Madry, S., Crumley, C., 1990. An application of remote sensing and GIS in a regional  
602 archaeological settlement pattern analysis: the Arroux River Valley, Burgundy, France, in:  
603 Allen, K., Green, S., Zubrow, E. (Eds.), *Interpreting Space: GIS and Archaeology*. Taylor  
604 and Francis, Bristol, PA.

605 Magnini, L., Bettineschi, C., De Guio, A., 2016. Object-based Shell Craters Classification from  
606 LiDAR-derived Sky-view Factor. *Archaeol. Prospect.* 24, 211–223.  
607 <https://doi.org/10.1002/arp.1565>

608 Mao, J., Jain, A.K., 1992. Texture classification and segmentation using multiresolution  
609 simultaneous autoregressive models. *Pattern Recognit.* 25, 173–188.  
610 [https://doi.org/10.1016/0031-3203\(92\)90099-5](https://doi.org/10.1016/0031-3203(92)90099-5)

611 Marquardt, W.H., 2010. Shell mounds in the southeast: middens, monuments, temple mounds,  
612 rings, or works? *Am. Antiq.* 75, 551–570. <https://doi.org/10.7183/0002-7316.75.3.551>

613 Matteson, M.R., 1960. Reconstruction of Prehistoric Environments through the Analysis of  
614 Molluscan Collections. *Am. Antiq.* 26, 117–120.

615 McKinley, A.C., 1921. Photos of the Cahokia Mounds. Exploration and fieldwork of the  
616 Smithsonian Institution in 1921. Smithsonian Institution, Washington D. C.

617 Moore, C.B., 1899. Certain aboriginal remains of the Alabama river. P.C. Stockhausen,  
618 Philadelphia.

619 Moore, C.B., 1894a. Certain sand mounds of the St. John’s River, Florida, Part I. *J. Acad. Nat.*  
620 *Sci. Phila.* 10, 1–103.

621 Moore, C.B., 1894b. Certain Sand Mounds of the St. John’s River, Florida, Part II. *J. Acad. Nat.*  
622 *Sci. Phila.* 10, 129–246.

623 Moorehead, W.K., 1891. Record of Warren K. Moorehead, Explorations, Little Miami Valley,  
624 Ohio, April 1891–Jan. 1892. (Field notes on file No. File A-17, Folder 6). Field Museum of  
625 Natural History, Chicago.

626 Nance, J.D., 1979. Regional Subsampling and Statistical Inference in Forested Habitats. *Am.*  
627 *Antiq.* 44, 172–176.

628 National Oceanic, and Atmospheric Administration, 2015. Sea Level Rise Adaptation Report  
629 Beaufort County, South Carolina (No. SCSGC-T-15-02).

630 Ozawa, K., 1978. Classification of the keyhole shaped tombs by template matching method.  
631 *IEEE Transactions on Computers* 27, 462–467.

632 Parcak, S.H., 2009. *Satellite Remote Sensing for Archaeology*. Routledge, New York.

633 Parrington, M., 1983. Remote Sensing. *Annu. Rev. of Anthropol.* 12, 105–124.

634 Prufer, K.M., Thompson, A.E., Kennett, D.J., 2015. Evaluating airborne LiDAR for detecting  
635 settlements and modified landscapes in disturbed tropical environments at Uxbenká, Belize.  
636 *J. Archaeol. Sci.* 57, 1–13. <https://doi.org/10.1016/j.jas.2015.02.013>

637 Putnam, F.W., 1875. List of items from mounds in New Madrid County, Missouri, and brief  
638 description of excavations, in: Harvard University, Peabody Museum, Eighth Annual  
639 Report. pp. 16–46.

640 Redfern, S., Lyons, G., Redfern, R.M., 1999. Digital elevation modelling of individual  
641 monuments from aerial photographs. *Archaeol. Prospect.* 6, 211–224.  
642 [https://doi.org/10.1002/\(SICI\)1099-0763\(199912\)6:4<211::AID-ARP125>3.0.CO;2-7](https://doi.org/10.1002/(SICI)1099-0763(199912)6:4<211::AID-ARP125>3.0.CO;2-7)

643 Redfern, S., Lyons, G., Redfern, R.M., 1998. The Automatic Morphological Description and  
644 Classification of Archaeological Monuments from Vertical Aerial Photographs, in:  
645 Proceedings of OEMI/IMVIP Joint Conference. Maynooth, Ireland.

646 Riley, M.A., 2009. Automated Detection of prehistoric conical burial mounds from LIDAR bare-  
647 earth digital elevation models (Master’s Thesis). Department of Geology and Geography,  
648 Northwest Missouri State University, Maryville, Missouri.

649 Russo, M., 2006. Archaic Shell Rings of the Southeast U.S.: National Historic Landmarks  
650 Historic Context. Southeast Archeological Center, National Park Service, Tallahassee.

651 Russo, M., 2004. Measuring Shell Rings for Social Inequality, in: Gibson, J.L., Carr, P.J. (Eds.),  
652 Signs of Power: The Rise of Cultural Complexity in the Southeast. University of Alabama  
653 Press, Tuscaloosa, pp. 26–70.

654 Saunders, R. (2004). Spatial Variation in Orange Culture Pottery: Interaction and Functions. In  
655 R. Saunders & C. Hays (Eds.), *Early Pottery, Technology, Function, Style, and Interaction*  
656 *in the Lower Southeast* (pp. 40–62). Tuscaloosa: University of Alabama Press.

657 Schaedel, R.P., 1951. The lost cities of Peru. *Sci. Am.* 185, 18–24.

658 Schiffer, M.B., Sullivan, A.P., Klinger, T.C., 1978. The design of archaeological surveys. *World*  
659 *Archaeol.* 10, 1–28.

660 Sevara, C., Pregesbauer, M., Doneus, M., Verhoeven, G., Trinks, I., 2016. Pixel versus object —  
661 A comparison of strategies for the semi-automated mapping of archaeological features  
662 using airborne laser scanning data. *J. Archaeol. Sci. Rep.* 5, 485–498.  
663 <https://doi.org/10.1016/j.jasrep.2015.12.023>

664 South, S., 1960. *An Archaeological Survey of Southeastern Coastal North Carolina*. Brunswick  
665 Town State Historic Site, Wilmington.

666 South, S., 1973. *An Archeological Survey of Jenkins Island Beaufort County, South Carolina*,  
667 Research Manuscript Series, No. 42. The South Carolina Institute of Archeology and  
668 Anthropology, University of South Carolina.

669 Squire, E.G., Davis, E.H., 1848. *Ancient monuments of the Mississippi Valley: comprising the*  
670 *results of extensive original surveys and explorations*. Smithsonian Institution.

671 Stark, B.L., Garraty, C.P., 2008. Parallel archaeological and visibility survey in the western  
672 Lower Papaloapan Basin, Veracruz. Mexico. *J. Field Archaeol.* 33, 177–196.

673 Stephenson, R.L., 1971. A basic inventory of archaeological sites in South Carolina, Research  
674 Manuscript Series. South Carolina Institute of Archaeology and Anthropology.

675 Swallow, G.C., 1858. Indian Mounds In New Madrid County, Missouri. *Transactions of the*  
676 *Academy of Science of St. Louis* 1, 36.

677 Thomas, C., 1894. Report on the Mound Explorations of the Bureau of Ethnology, Annual  
678 Report of the Bureau of American Ethnology, vol. 12. Smithsonian Institution, Washington  
679 D. C.

680 Thompson, A.E., Prufer, K.M., 2015. Airborne LiDAR for detecting ancient settlements and  
681 landscape modifications at Uxbenka, Belize. *Res. Rep. Belizean Archaeol.* 12, 251–259.

682 Thompson, V.D., Arnold, P.J., Pluckhahn, T.J., VanDerwarker, A.M., 2011. Situating Remote  
683 Sensing in Anthropological Archaeology. *Archaeol. Prospect.* 18, 195–213.  
684 <https://doi.org/10.1002/arp.400>

685 Trier, Ø.D., Larsen, S.Ø., Solberg, R., 2008. Detection of circular patterns in high-resolution  
686 satellite images of agricultural land with CultSearcher (No. SAMBA/16/08). Norsk  
687 Regnesentral, Oslo.

688 Trier, Ø.D., Pilø, L.H., 2012. Automatic Detection of Pit Structures in Airborne Laser Scanning  
689 Data: Automatic detection of pits in ALS data. *Archaeol. Prospect.* 19, 103–121.  
690 <https://doi.org/10.1002/arp.1421>

691 Trier, Ø.D., Zortea, M., 2012. Semi-automatic detection of cultural heritage in lidar data, in:  
692 *Proceedings of the 4th GEOBIA*, May 7-9. Rio de Janeiro, p. 123.

693 Trier, Ø.D., Zortea, M., Tønning, C., 2015. Automatic detection of mound structures in airborne  
694 laser scanning data. *J. Archaeol. Sci. Rep.* 2, 69–79.  
695 <https://doi.org/10.1016/j.jasrep.2015.01.005>

696 Trimble, 2016. eCognition version 9.2.1. Trimble Germany GmbH, Munich, Germany

697 Trinkley, M.B., 1981. Studies of Three Woodland Period Sites in Beaufort County, South  
698 Carolina. SC Department of Highways and Public Transportation.

699 Trinkley, M.B., 1985. The Form and Function of South Carolina's Early Woodland Shell Rings,  
700 in: Dickens, R.S., Ward, H.T. (Eds.), *Structure and Process in Southeastern Archaeology*.  
701 University of Alabama Press, Tuscaloosa, pp. 102–118.

702 Vaze, J., Teng, J., Spencer, G., 2010. Impact of DEM accuracy and resolution on topographic  
703 indices. *Environ. Model. Softw.* 25, 1086–1098.  
704 <https://doi.org/10.1016/j.envsoft.2010.03.014>

705 Walker, M.P., 2016. *Tracking Trajectories: Charting Changes of Late Archaic Shell Ring*  
706 *Formation and Use* (Master's Thesis). University of Tennessee, Knoxville.

707 Wauchope, R., 1948. The Ceramic Sequence in the Etowah Drainage, Northwest Georgia. *Am.*  
708 *Antiq.* 13, 201–209.

709 Weishampel, J., Hightower, J., Chase, A., Chase, D., Patrick, R., 2011. Detection and  
710 Morphologic Analysis of Potential Below-Canopy Cave Openings in the Karst Landscape  
711 around the Maya Polity of Caracol using Airborne Lidar. *J. Cave and Karst Stud.* 73, 187–  
712 196. <https://doi.org/10.4311/2010EX0179R1>

713 Willey, G.R., 1939. Ceramic Stratigraphy in a Georgia Village Site. *Am. Antiq.* 5, 140–147.

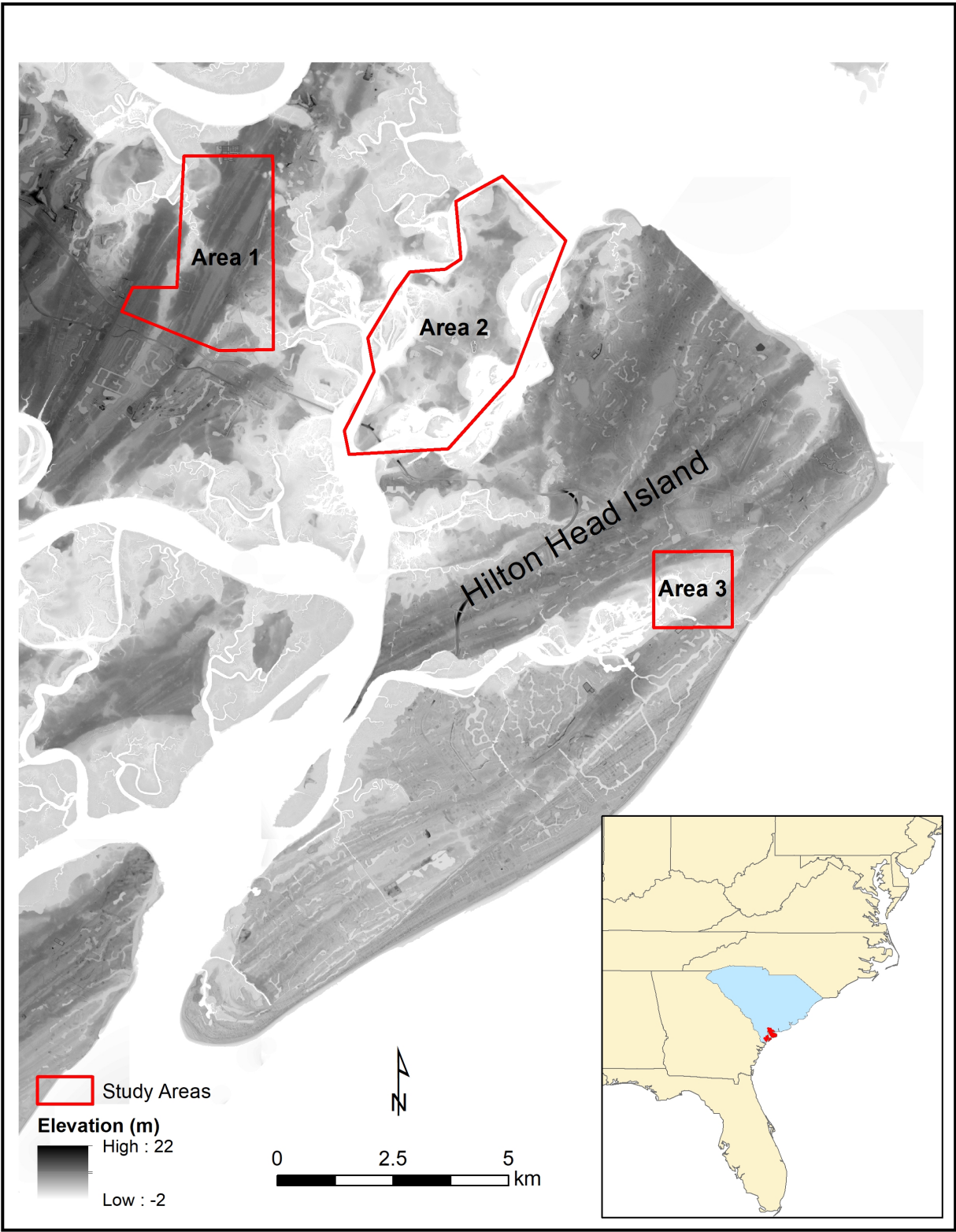
714 Williams-Hunt, P.D.R., 1950. Irregular earthworks in eastern Siam: an air survey. *Antiquity* 24,  
715 30–36.

716 Witharana, C., Ouimet, W.B., Johnson, K.M., 2018. Using LiDAR and GEOBIA for automated  
717 extraction of eighteenth–late nineteenth century relict charcoal hearths in southern New  
718 England. *GIScience & Remote Sens.* 1–22. <https://doi.org/10.1080/15481603.2018.1431356>

719 Wu, Q., Deng, C., Chen, Z., 2016. Automated delineation of karst sinkholes from LiDAR-  
720 derived digital elevation models. *Geomorphology* 266, 1–10.

721 Wu, Q., Liu, H., Wang, S., Yu, B., Beck, R., Hinkel, K., 2015. A localized contour tree method  
722 for deriving geometric and topological properties of complex surface depressions based on  
723 high-resolution topographical data. *Int. J. Geogr. Inf. Sci.* 29, 2041–2060.  
724 <https://doi.org/10.1080/13658816.2015.1038719>

725 Yokoyama, R., Shirasawa, M., Pike, R.J., 2002. Visualizing Topography by Openness: A New  
726 Application of Image Processing to Digital Elevation Models. *Photogramm. Eng. Remote*  
727 *Sens.* 68, 257–266.



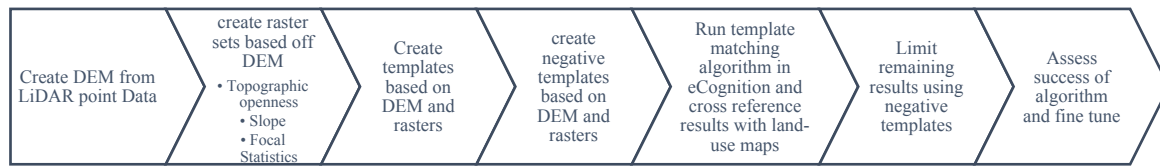
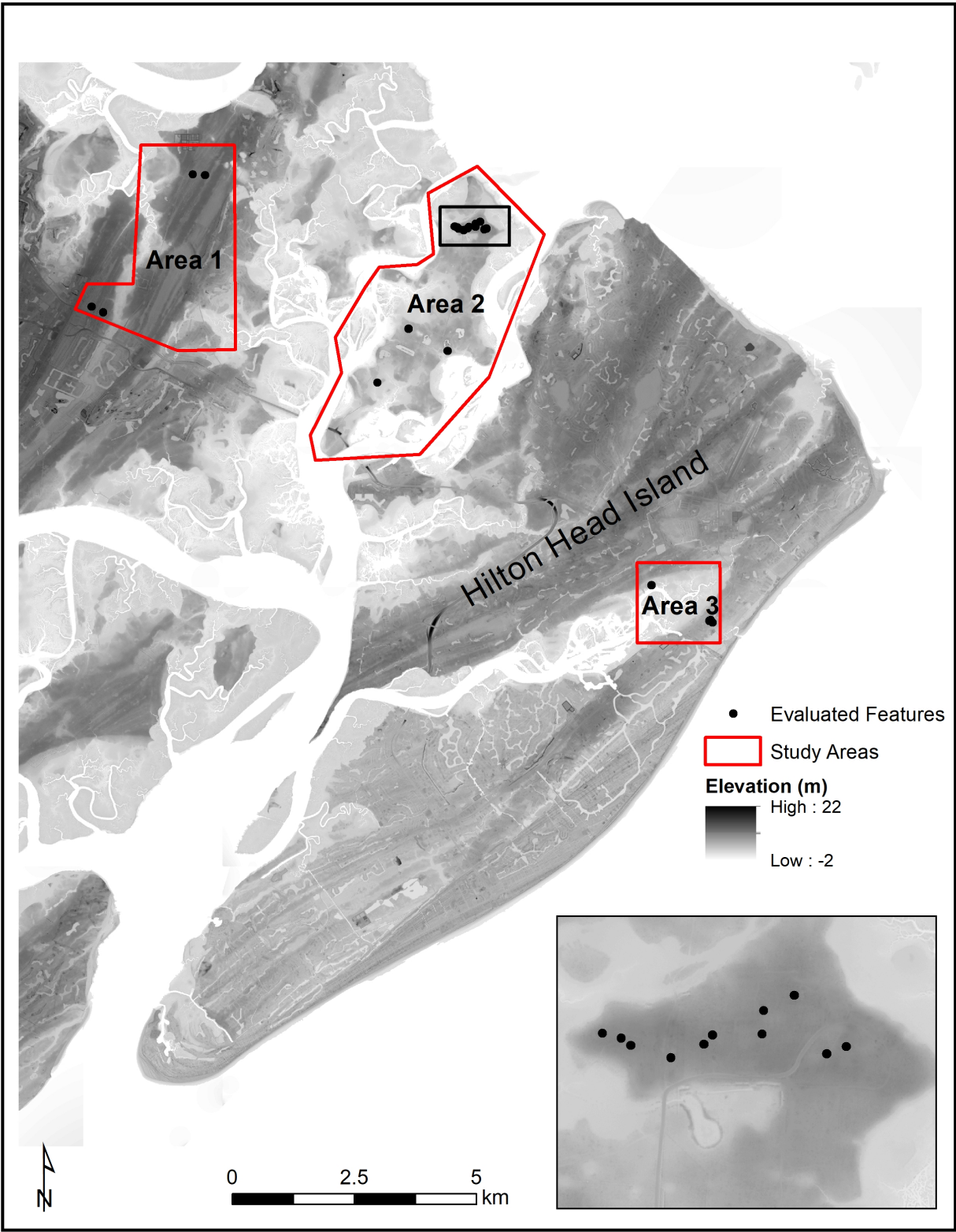
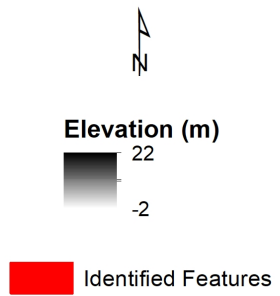
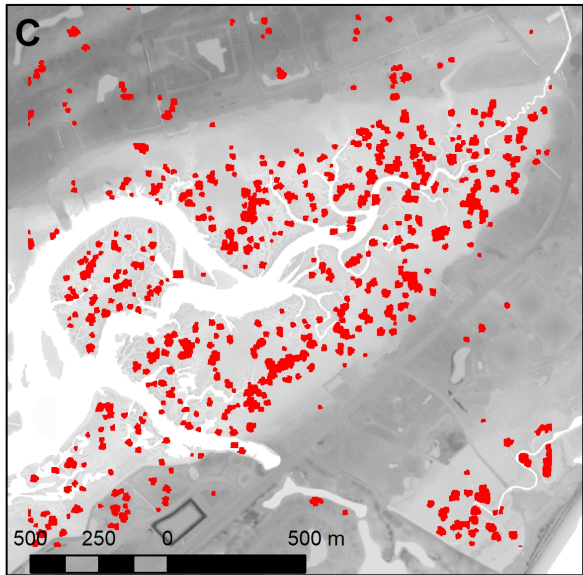
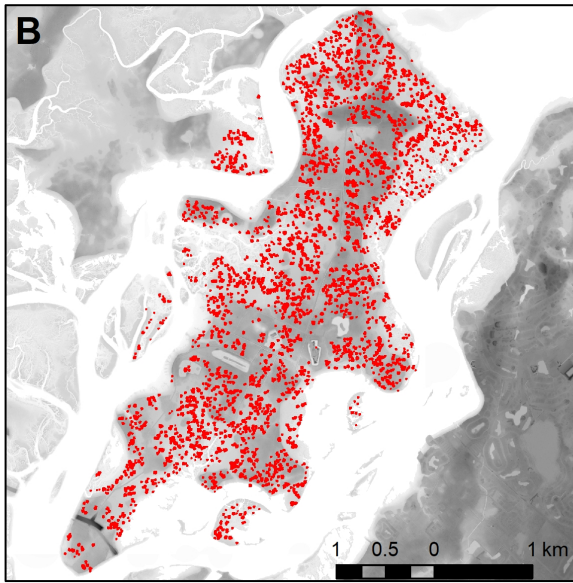
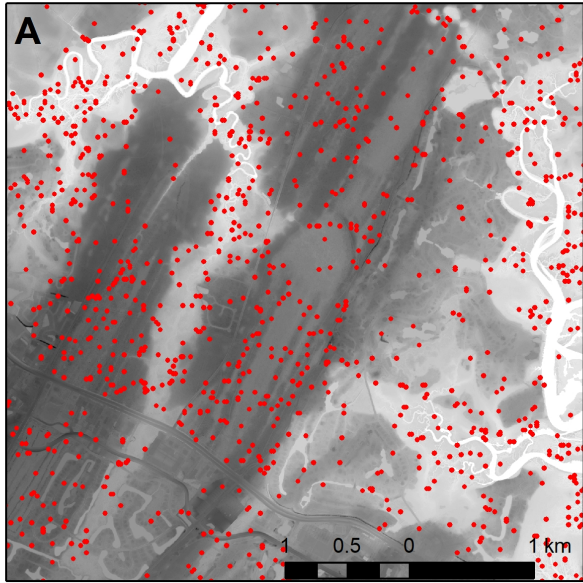
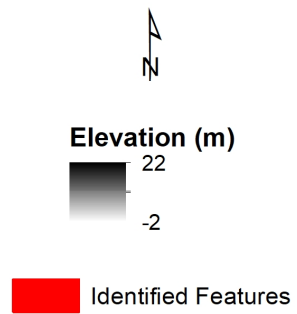
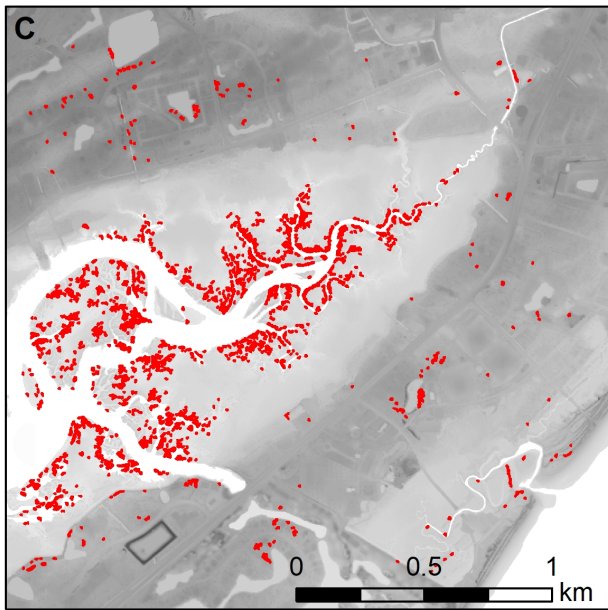
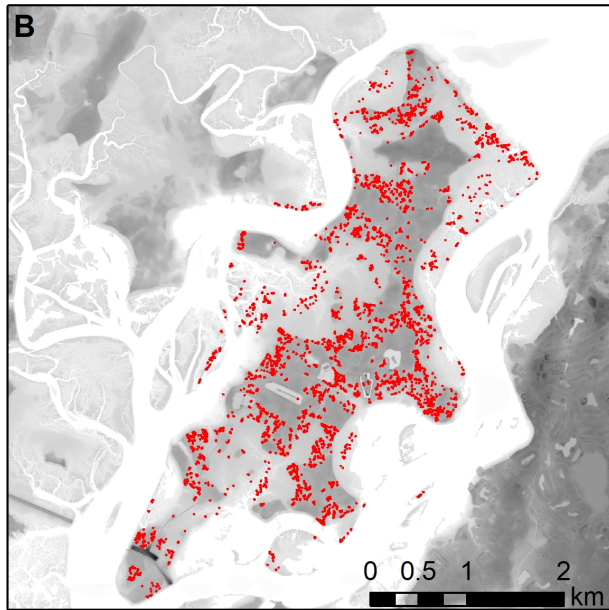
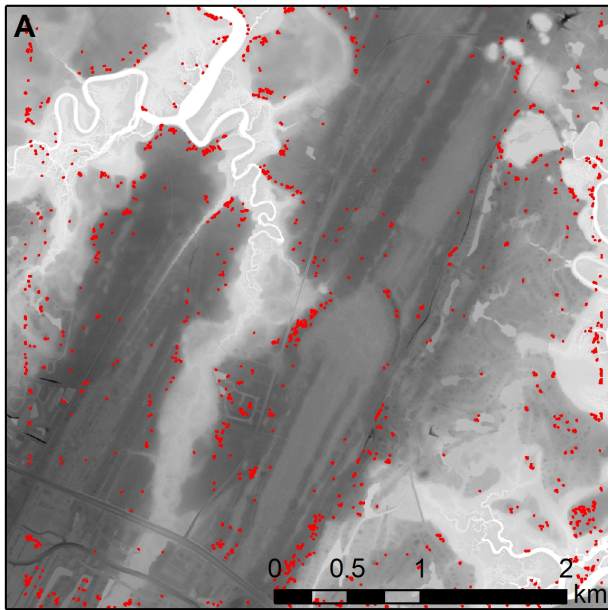
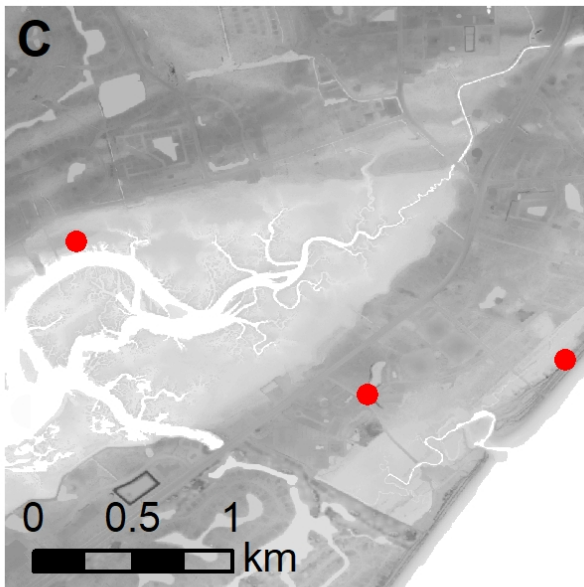
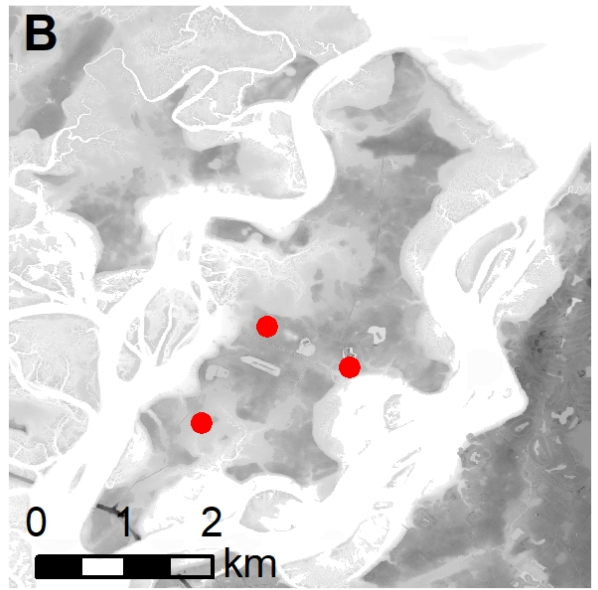
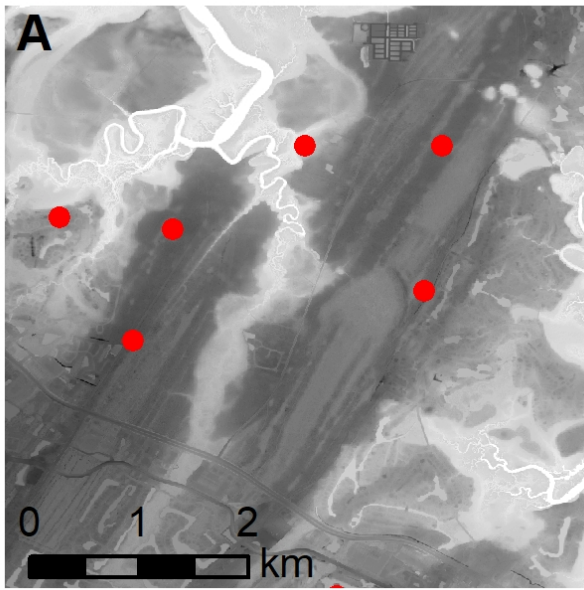


Figure 2: Steps involved in the use of template matching for the identification of mound features.



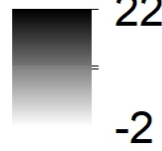






● Identified Features

**Elevation (m)**



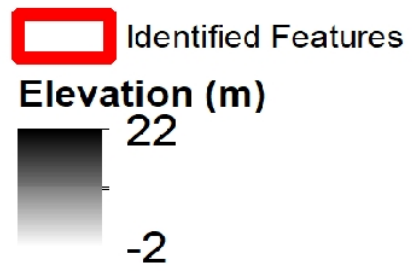
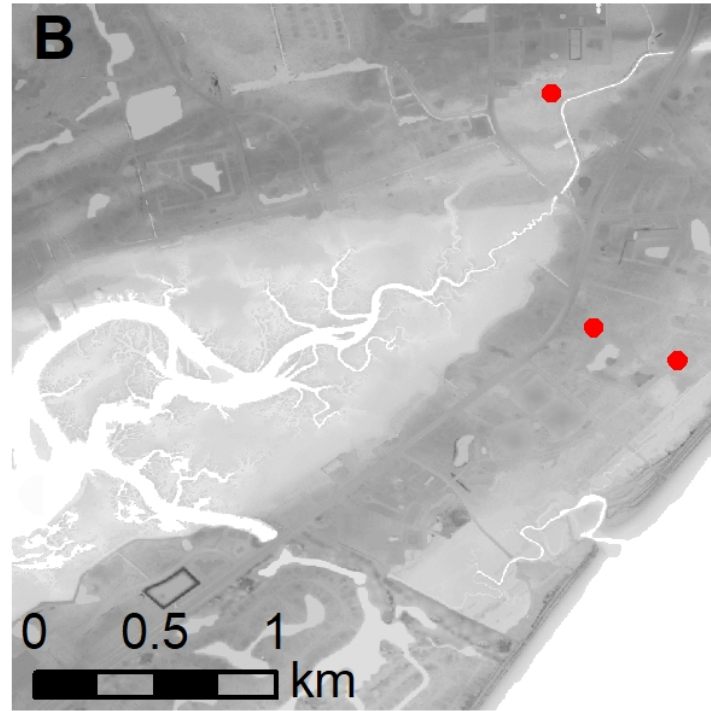
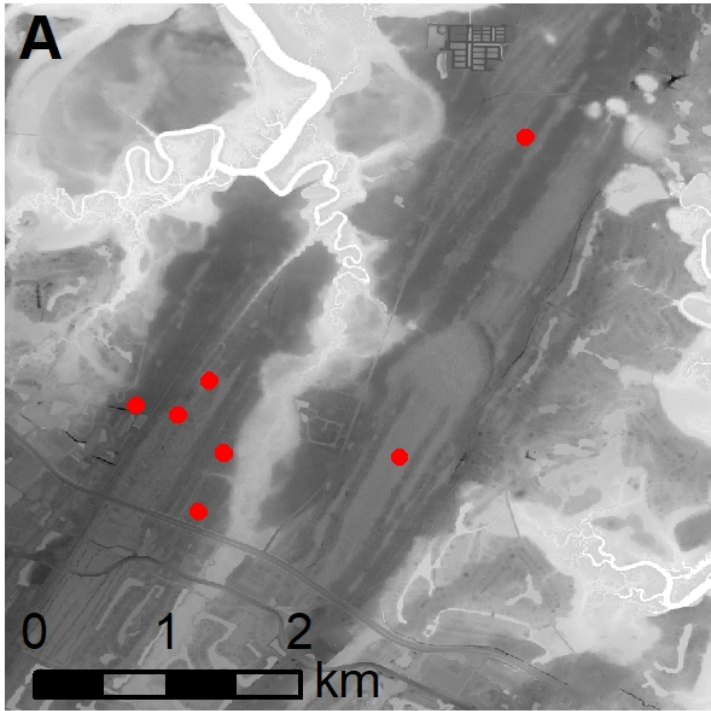


Table 1: Parameters used in multiresolution segmentation of the Beaufort County LiDAR data.

<i>Parameter</i>	<i>Threshold</i>
Area	$\leq 150 \text{ m}^2$
Circularity	$\geq 0.6$
Asymmetry	$0 - 0.3$
Compactness	$\geq 1.0$

Table 2: Total detections made by each OBIA technique.

OBIA Method	Total Detections	Total Detections	Total Detections
	Study Area 1	Study Area 2	Study Area 3
Segmentation	1,399	1,091	380
IDA (100 iterations)	3,332	1,677	413
IDA (200 iterations)	1,582	1,829	807
IDA (300 iterations)	1,093	2,485	817
Template Matching	6	3	3
Combined	7	0	3

Table 3: OBIA Method Results from Field Survey

OBIA Method	Sites Surveyed	Accurate identifications determined by field survey	False Positives determined by field survey	Rate of positive identification/false positives based on field survey	Total Detections in Study Areas	Potential new mound features
Segmentation Classification	12	6	6*	1:1	2,490	1,245
IDA (100 iterations)	14	5	9**	5:9	5,422	3,012
TM	6	3	3	1:1	10	5
Combined (segmentation and TM)	4	4	0	1:0	10	10

\* Two sites were inconclusive  
\*\* One site was inconclusive

Table 4: Change in detection accuracy for known archaeological deposits in Area 2 using increasing numbers of iterations. As the number of iterations increases, so too does the number of identified archaeological deposits.

<b>Number of Iterations</b>	<b>Number of Identified Archaeological Deposits</b>
<b>100</b>	40
<b>200</b>	59
<b>300</b>	60

Table 5: Overall accuracy for IDA using increasing numbers of iterations. As the number of iterations increases, the number of false positive detections decreases, and the overall accuracy increases.

<b>Number of Iterations</b>	<b>True Positive Identifications (Determined by ground-survey)</b>	<b>False Positive Identifications (Determined by ground-survey)</b>	<b>Total Detections</b>	<b>Overall Accuracy</b>
<b>100</b>	5	9	5,422	35.71%
<b>200</b>	3	3	4,218	50.00%
<b>300</b>	5	2	4,395	71.43%

Table 6: Archaeological utility of OBIA methods. Topographic discrimination refers to each method’s ability to distinguish between natural and anthropogenic features. Archaeological detection accuracy refers to the ratio of positive detections to false ones. Overall utility is the average of the topographic discrimination and archaeological detection accuracies.

METHOD	Segmentation	IDA (100 iterations)	IDA (200 iterations)	IDA (300 iterations)	TM	Combined
Topographic Discrimination Accuracy	50%	57.14%	66.67%	85.71%	100%	100%
Archaeological Detection Accuracy	50%	35.71%	50%	71.43%	50%	100%
<b>Overall Utility (average of accuracies)</b>	<b>50%</b>	<b>46.43%</b>	<b>58.34%</b>	<b>78.57%</b>	<b>75%</b>	<b>100%</b>

Supplemental Table 1: List of Sites on Pinckney Island (Study Area 2) identified by IDA and Segmentation. Template matching and the combined method did not identify any pre-identified archaeological deposits. An *I* indicates that the method identified that site. If a method did not identify a site, the column is left blank.

SITEID	IDA (100 Iterations)	IDA (200 Iterations)	IDA (300 Iterations)	Segmentation
38BU0092		/		/
38BU0653		/	/	/
38BU0092		/		/
38BU0092		/	/	/
38BU0093	/	/	/	/
38BU0094	/	/	/	
38BU0095	/		/	/
38BU0066	/	/	/	/
38BU0067	/	/	/	
38BU0068		/		/
38BU0069		/		/
38BU0193	/	/	/	/
38BU0193	/	/	/	/
38BU0069	/	/	/	/
38BU0069	/	/	/	/
38BU0166				/
38BU0168	/	/	/	/
38BU0169	/		/	/
38BU0170	/			
38BU0172				/
38BU0173	/	/	/	
38BU0174	/		/	/
38BU0175		/		
38BU0176	/	/	/	/
38BU0177		/	/	/
38BU0180	/		/	
38BU0181	/	/	/	/
38BU0182	/	/		/
38BU0183	/	/	/	/
38BU0185	/	/		/
38BU0186				/
38BU0187	/	/	/	/
38BU0188	/		/	
38BU0191	/		/	/
38BU0192	/			/
38BU0194				/
38BU0195	/	/	/	/
38BU0198				/
38BU0199	/		/	/

38BU0201	/			/
38BU0202				/
38BU0203		/		/
38BU0204		/	/	/
38BU0205	/	/	/	/
38BU0206	/	/	/	/
38BU0208	/	/	/	/
38BU0209		/	/	/
38BU0210		/	/	/
38BU0211		/		
38BU0212		/	/	/
38BU0213	/	/	/	/
38BU0214				/
38BU0215			/	/
38BU0216		/		
38BU0217		/		/
38BU0368				/
38BU0664	/		/	
38BU0665	/		/	/
38BU0668				/
38BU0669				/
38BU0670				/
38BU0672		/		
38BU0673	/			/
38BU0674				/
38BU0470				/
38BU0471		/	/	/
38BU0694		/	/	/
38BU0694		/	/	/
38BU0471		/	/	/
38BU0472	/	/	/	/
38BU0473	/	/	/	/
38BU0474	/	/	/	/
38BU0650		/	/	/
38BU0651	/	/	/	/
38BU0652	/	/	/	/
38BU0654	/		/	/
38BU0656	/	/	/	/
38BU0657				/
38BU0658			/	/
38BU0661			/	/
38BU0662	/	/	/	/
38BU0675	/	/	/	/
38BU0676		/	/	/

38BU0677			/	/
38BU0678				/
38BU0693	/		/	/
38BU0696		/		/
38BU0699				/
38BU0700	/		/	
38BU0702	/	/	/	/
38BU0703	/	/	/	/
38BU0704				/
38BU0705	/	/	/	/
38BU0706		/		/
38BU0707	/	/	/	/
38BU0710		/		/
38BU1215		/		
<b>TOTAL</b>	<b>49</b>	<b>59</b>	<b>60</b>	<b>84</b>